



저작자표시-비영리-변경금지 2.0 대한민국

이용자는 아래의 조건을 따르는 경우에 한하여 자유롭게

- 이 저작물을 복제, 배포, 전송, 전시, 공연 및 방송할 수 있습니다.

다음과 같은 조건을 따라야 합니다:



저작자표시. 귀하는 원저작자를 표시하여야 합니다.



비영리. 귀하는 이 저작물을 영리 목적으로 이용할 수 없습니다.



변경금지. 귀하는 이 저작물을 개작, 변형 또는 가공할 수 없습니다.

- 귀하는, 이 저작물의 재이용이나 배포의 경우, 이 저작물에 적용된 이용허락조건을 명확하게 나타내어야 합니다.
- 저작권자로부터 별도의 허가를 받으면 이러한 조건들은 적용되지 않습니다.

저작권법에 따른 이용자의 권리는 위의 내용에 의하여 영향을 받지 않습니다.

이것은 [이용허락규약\(Legal Code\)](#)을 이해하기 쉽게 요약한 것입니다.

[Disclaimer](#)

A THESIS
FOR THE DEGREE OF DOCTOR OF PHILOSOPHY

Marine-derived bioactive compound regulates obesity through
leptin signaling pathway

Nalae Kang

Department of Marine Life Science
GRADUATE SCHOOL
JEJU NATIONAL UNIVERSITY

August, 2016

Marine-derived bioactive compound regulates obesity through leptin signaling pathway


Nalae Kang

(Supervised by Professor You-Jin Jeon)

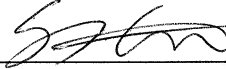
A thesis submitted in partial fulfillment of the requirement
for the degree of DOCTOR OF PHILOSOPHY

2016. 08.


This thesis has been examined and approved by



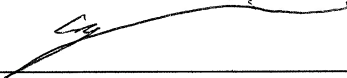
Thesis director, Gi-Young Kim, Prof. of Marine Life Science
Jeju National University




Seung-Hong Lee, Prof. of Food Bio Science
Konkuk University



Soo-Jin Heo, Ph.D.-senior researcher
Korea Institute of Ocean Science and Technology



Seunghoon Lee, Prof. of Marine Life Science
Jeju National University



You-Jin Jeon, Prof. of Marine Life Science
Jeju National University

2016. 08.
Date

**Department of Marine Life Science
GRADUATE SCHOOL
JEJU NATIONAL UNIVERSITY**

CONTENTS

국문초록	iv
------------	----

ABSTRACT	xi
----------------	----

LIST OF FIGURES.....	xvi
----------------------	-----

PART 1. Screening of marine-derived bioactive compounds for leptin receptor agonist and its validation in *in vitro*

Abstract	2
-----------------------	----------

Introduction	3
---------------------------	----------

Materials and methods.....	6
-----------------------------------	----------

<i>In silico</i> docking of new inhibitor candidates to proteins	6
------------------------------------------------------------------------	---

Molecular docking analysis of candidate compounds on ObR.....	6
---------------------------------------------------------------	---

Chemicals and reagents.....	7
-----------------------------	---

Cell culture.....	7
-------------------	---

Cytotoxicity.....	7
-------------------	---

Assay for leptin signaling pathway.....	8
-----------------------------------------	---

Immunoblotting.....	8
---------------------	---

Statistical analysis	9
Results and discussion	10
 PART 2. Appetite control effects of octaphlorethol A in central nervous system in obese mice fed with high fat diet	
Abstract	24
Introduction	25
Materials and methods	27
Chemicals and reagents.....	27
Animals	27
Frozen block tissue slide	28
Cresyl violet staining	28
Immunohistochemistry	28
Statistical analysis	29
Results and discussion	30
 PART 3. Effects of octaphlorethol A on peripheral metabolism as leptin substitute in obese mice fed with high fat diet	

Abstract	40
Introduction	41
Materials and methods	43
Chemicals and reagents.....	43
Animals	43
Measurement of serum parameters	44
Paraffin block tissue slide	44
Frozen block tissue slide	44
Hematoxylin and eosin staining.....	44
Immunohistochemistry	45
Statistical analysis	45
Results and discussion	46
CONCLUSION	73
REFERENCE	74

국문초록

현대 질병-비만

서구화된 식습관을 비롯한 운동의 부족, 과도한 업무로 인한 스트레스 등의 사회적 변화는 다양한 현대 질병을 야기하였다. 체내 에너지 대사의 불균형에 따라 발생하는 비만, 당뇨, 고혈압과 같은 대사성 질환이 대표적인 현대 질병이다. 특히 비만은 과거에는 외형적, 미용적 문제로만 여겨졌으나 최근 전 세계적으로 비만 발생률이 높아지고 있으며, 과체중이나 비만을 넘어서 고도비만에 이르러 문제가 심각해지면서 점차 질병으로 인식되고 있다. 이에 따라 세계보건기구에서는 비만을 '건강에 해가 될 정도로 비정상적이거나 과도하게 지방이 축적된 상태'라고 정의하였으며, '21세기 신종 전염병'이라고 지목하면서 그 위험성에 대하여 경고하고 있다.

비만의 지표

성인의 과체중 또는 비만을 구분하는 지표로서 체질량지수 (Body Mass Index; BMI)가 가장 보편적으로 사용되고 있으며, 이 수치는 신장(m)의 제곱에 대한 체중(kg/m²)을 나타낸다. 세계보건기구에서는 인종이나 성별에 관계없이 체질량지수 25 kg/m² 이상을 과체중, 30 kg/m² 이상을 비만으로 정의하였다. 그러나 우리나라를 비롯한 아시아인의 경우 체질량지수 25 kg/m²를 시점으로 비만 관련 질환 발병률이 1.5~2 배로 증가하며, 그 이하에서도 비만과 연관되어 있다고 알려진 당뇨병 및 심혈관계질환 위험이 나타나고 있다. 또한 동일한 체질량지수에서 서양인에 비해 상대적으로 복부지방과 체지방률이 높다. 따라서 세계보건기구 아시아태평양 지역과 대한비만학회에서는 아시아인의 과체중의 기준을 체질량지수 23 kg/m² 이상, 비

만의 기준을 25 kg/m^2 이상으로 정의하고 있다.

비만 문제의 심각성-비만 유병률 및 비만 합병증

세계보건기구에서 2016년 6월에 발표한 보고에 따르면 2014년에 전 세계 성인 (18세 이상) 19억 명 이상이 과체중이며, 이 중 6억 명 이상이 비만인 것으로 나타났다. 이는 전 세계 18세 이상 성인의 39%가 과체중이고, 13%가 비만을 의미한다. 또한 4천 1만 명의 5세 이하의 어린이들이 과체중 또는 비만인 것으로 나타났다. 이러한 세계 비만 유병률은 1980년보다 2배 이상 증가한 수치이다. 우리나라의 만 19세 이상 성인의 비만 유병률도 1998년 26.0%에서 2013년 31~32%로 증가하였고, 특히 남성의 비만 유병률은 35~37%인 것으로 나타나 여성보다 남성의 비만 유병률이 높다고 보고되었다 (2013 국민건강통계, 보건복지부).

한편, 비만 인구의 증가와 함께 제 2형 당뇨병 및 대사증후군의 발병률이 증가하고 있다. 비만은 인슐린 저항성을 일으켜 대사 합병증인 이상지질혈증, 고혈압, 당대사 장애, 당뇨병, 죽상동맥경화증, 심혈관계 질환, 뇌졸중, 담낭질환, 신장질환, 간기능 부전, 근골격계 질환, 관절염, 수면장애, 악성신생물 등의 각종 합병증을 야기한다. 또한 BMI가 $35\sim40 \text{ kg/m}^2$ 인 경우 사망위험이 정상인보다 2~8 배 높으며, 고도비만 ($> 40 \text{ kg/m}^2$)환자의 사망률은 정상인보다 12배 높다.

비만의 치료-비만치료제

비만 치료를 위해서는 생활 습관을 개선하는 생활요법이 가장 중요하지만, 생활 습관 개선이 어렵거나 비만의 정도가 심한 경우, 비만 치료를 돕기 위해 여러 가지 비만치료제가 개발되어 판매되고 있다. 일반적으로 비만치료제는 약물 기전에 따라

크게 지방흡수저해제와 식욕억제제로 구분할 수 있다.

현재 상용되고 있는 비만치료제의 종류로는 1994년 4월에 미국 FDA (Food and Drug Administration)의 승인을 받아 최초로 공인받은 약제로 기록되고 있는 올리스타트 (Orlistat)와 2012년에 승인을 받은 펜터민/토피라메이트 병합제 (Phentermine/topiramate; Qsymia)와 로카세린 (Lorcaserin; Belviq), 2014년에 승인을 받은 날트렉손/부프로피온 병합제 (Naltrexone/bupropion; Contrave)가 있다. 올리스타트 (Orlistat)와 함께 기존에 사용되던 시부트라민 (Sibutramine)은 심혈관질환 또는 당뇨병이 있는 환자를 대상으로 시행한 연구에서 혈압과 맥박을 증가시키고, 관상 동맥질환, 울혈성 심부전, 부정맥, 뇌졸중 등의 심혈관질환이 발생하는 부작용을 보여, 2010년 10월 이후로 전 세계적으로 사용이 중단되었다.

올리스타트 (Orlistat)는 지방분해효소인 췌장의 라이페이스 (lipase) 억제제로서 음식물에 포함된 지방의 분해 및 흡수를 억제한다. 따라서 섭취한 지방의 약 30%는 소화 및 흡수되지 않고 그대로 몸 밖으로 배출된다. 반면, 펜터민/토피라메이트 병합제 (Phentermine/topiramate)의 펜터민 (Phentermine), 로카세린 (Lorcaserin), 날트렉손/부프로피온 (Naltrexone/bupropion)은 식욕억제 기전을 갖는 비만치료제이다. 펜터민 (Phentermine)은 흥분성 신경전달물질 분비를 통해 식욕을 억제하는 약물이고, 로카세린 (Lorcaserin)은 세로토닌 계열의 식욕억제제로서 세로토닌_{2C}수용체 (5-HT_{2C} receptor)에 선택적으로 작용하는 약물이다. 날트렉손과 부프로피온 (Naltrexone/bupropion)은 시상하부와 중뇌 변연계 (Limbic system)의 보상중추에 작용하는 식욕억제제이다.

비만치료제의 부작용

이러한 약물들은 전임상 및 임상연구를 통해 항비만 효과가 검증되어 있지만, 약물의 기전에 따라 메스꺼움, 불면증, 소화 불량, 심혈관질환, 정신질환 등의 여러 가지 부작용도 나타나고 있다. 또한 올리스타트 (Orlistat)를 제외하고 최근 FDA의 허가를 받은 비만치료제의 경우, 임상 연구기간이 2년 정도로 짧아 장기간 복용시의 안전성에 대한 연구가 부족한 실정이다. 그럼에도 불구하고 환자의 상태를 고려하지 않거나, 관리기관의 권고 사항을 무시한 비만치료제의 오남용 또는 과다처방으로 심각한 부작용의 사례가 발생하고 있다.

현재 상용중인 식욕억제제의 문제점

특히 현재 상용되고 있는 몇몇 식욕억제제는 근본적인 식욕억제 기전을 따르는 약제가 아니라, 뇌에서 배고픔을 덜 느끼게 하거나, 포만감을 느끼게 하는 기전으로 마약류 (향정신성의약품)로 분류되어 있다. 이는 약제 의존성이나 내성이 발생할 수 있으며, 두근거림, 혈압상승, 가슴통증, 현기증, 불안, 초조, 불면, 흥분 등에서부터 장기간 복용할 경우, 폐동맥 고혈압, 심장질환, 정신분열 등의 심각한 부작용이 나타날 수 있다.

근본적 식욕억제의 기전-렙틴 (Leptin)

식욕의 항상성은 그렐린 (Ghrelin)과 렙틴 (Leptin)이라는 두 가지의 호르몬이 관여하는데, 위 (Stomach)에서 분비되는 그렐린 (Ghrelin)에 의해 식욕자극 및 에너지 대사 억제가 일어나고, 지방 (Fat)에서 분비되는 렙틴 (Leptin)에 의해 식욕억제 및 에너지 대사가 일어난다. 각 조직에서 그렐린 (Ghrelin) 또는 렙틴 (Leptin)이 분비되면, 뇌의 시상하부에서 식욕 기능을 담당하는 프로오피오멜라노코르틴

(Proopiomelanocortin, POMC) 신경세포와 아구티-관련 펩타이드 (Agouti-related peptide, AgRP) 신경세포에 존재하는 각각의 수용체 (Receptor)에 작용하여 신호를 일으킨다. 대개의 비만 환자의 경우, 혈중 렙틴 (Leptin)의 수치가 정상범위를 초과하는 렙틴저항성 (Leptin resistance)을 나타낸다. 이는 지방세포에서 분비된 렙틴 (Leptin)이 렙틴 수용체에 결합하고, 그 신호가 세포 내로 전달되는 각 단계에서의 구조적 결함에 의해 발생하는 것으로 알려져 있다. 그러나 렙틴저항성 (Leptin resistance)이 식욕 억제를 방해하고 비만을 유발하는 중요한 원인임에도 불구하고 이를 개선하는 비만 치료제 연구 개발이 부족한 실정이다.

식의약소재로서의 해양생물자원의 가치

해양은 지구 전체 면적의 70%를 차지하고 있으며, 지구 생물종의 80%가 해양에 서식하는 생물 자원의 보고이다. 또한 해양생물은 육상생물과는 전혀 다른 환경에서 서식하여 다양한 자기방어 기제로 구조적으로 특이하고 다양한 2차 대사산물을 생산한다. 이러한 천연물은 합성 의약품과 달리 부작용이 없기 때문에 최근 신의약품 소재 개발 연구에 활용되고 있다.

해조류에는 미네랄, 비타민, 다당류 및 폴리페놀이 풍부하게 함유되어 있다. 특히 해조류의 폴리페놀은 항산화, 항암, 항염, 항염증 등 다양한 활성 성분이 알려져 있다. 하지만 육상식물 유래의 폴리페놀의 대사성질환 치료제, 비만, 당뇨, 고혈압에 대한 치료제로써의 연구는 다양한 방면에서 연구되고 있으나 해조류에서의 폴리페놀의 대사성 질환 치료제로써의 연구는 미흡한 실정이다.

연구의 목적

따라서 이 연구에서는 비만 개선 및 치료물질로서 렙틴/렙틴리셉터의 작용을 이용한 해양 천연물 유래 신의약 소재를 탐색하였다. 이를 위하여 제주 자생 해조류에서 분리된 다양한 플로로탄닌 (phlorotannin) 계열의 컴파운드를 대상으로 leptin signaling pathway를 통한 항비만 효과를 검증하여 기능성 의약품 소재로서의 개발 가능성을 확인하였다.

Part 1에서는 *in silico* study를 통하여 총 13가지 컴파운드를 대상으로 Leptin receptor의 결합부위에 대한 ligands 결합 친화도 (docking energy)를 비교 분석하였으며, 이 중 가장 높은 결합 친화도를 나타내는 컴파운드를 선정하였다. 또한 선정된 컴파운드의 leptin signaling pathway를 통한 식욕억제 효과를 검증하기 위하여 Leptin signal이 일어나는 주요 세포인 hypothalamic N1 neuron cell을 실험에 사용하였다.

Part 2에서는 Part 1의 연구결과로 선정된 compound의 Leptin signal을 통한 식욕억제 효과를 *in vivo* study로서 검증하였다. 동물은 C57BL/6J를 사용하였고, 총 10주의 실험 기간 동안 45 kcal 고지방 사료를 급여하여 비만을 유도하였다. 사료 급여 6주 후부터는 선정된 compound를 2.5 mg/kg으로 매일 경구투여하였다. 실험 종료 후, 동물을 희생하여 식욕억제 신호가 일어나는 조직인 뇌를 분리 적출하여 leptin signal의 중요한 molecules의 변화를 확인하였다.

Part 3에서는 Part 1의 연구결과로 선정된 compound의 Leptin signal을 통한 말초 조직의 에너지 대사 조절 효과를 *in vivo* study로 확인하였다. 동물은 C57BL/6J를 사용하였고, 총 10주의 실험 기간 동안 45 kcal 고지방 사료를 급여하여 비만을 유도하였다. 사료 급여 6주 후부터는 선정된 compound를 2.5 mg/kg으로 매일 경구투여하였다. 실험 종료 후, 동물을 희생하여 에너지 대사가 일어나는 조직인 백색

지방, 간, 근육을 분리 적출하였다. 이후, 지방의 크기, 지방간염, 근육 조직 등을 확인함으로써 에너지 대사의 조절을 확인하였으며, 렙틴 신호의 변화를 확인함으로써 에너지 대사와 렙틴 신호의 상호작용을 확인하였다.

ABSTRACT

Obesity

Overweight and obesity are conditions that results in an abnormal or excessive fat accumulation that might have a negative effect on human health (<http://www.who.int/mediacentre/factsheets/en/>). In normal physiological condition, the body weight is maintained by keeping an energy balance between intake and expenditure. Failure of the energy homeostasis, however, increases the body weight, and eventually leads to overweight and obesity (Klok, Jakobsdottir, & Drent, 2007).

Body mass index (BMI) is a commonly used parameter to classify overweight and obesity in adults. BMI is defined as a body weight in kilograms divided by the square of height in meters (kg/m^2). World Health Organization (WHO) defines overweight and obesity by using following BMI levels; a BMI ≥ 25 is overweight, a BMI ≥ 30 is obesity.

Worldwide obesity rate

Recently, obesity is rapidly increasing around the world and that has affected on both gender and age (Sáinz, Barrenetxe, Moreno-Aliaga, & Martínez, 2015). The worldwide prevalence of obesity has more than doubled between 1980 and 2014. According to the WHO report estimated in 2014, more than 1.9 billion adults, aged 18 years and older, were overweight. Among them, over 600 million were found to be obese. By definition, 39% of adults were overweight and 13% of them were obese. Moreover, 42 million children, under the age of 5, were overweight or obese in 2013.

Complications of obesity

Obesity is closely associated with various metabolic disorders including dyslipidemia, cardiovascular disease, stroke, insulin resistance, and type 2 diabetes (Zhou & Rui, 2013). Chronic inflammation in adipose tissues may play a critical role in the development of obesity-related metabolic dysfunctions. Thus, obesity increases the risk of developing a variety of pathological conditions, including insulin resistance, dyslipidemia, type 2 diabetes, nonalcoholic fatty liver disease (NAFLD), hypertension, coronary heart disease, ischemic stroke and several cancer conditions. (Ladenheim, 2015), (Jung & Choi, 2014), (R. Yang & Barouch, 2007).

Cause of obesity: imbalance

The fundamental cause of obesity and overweight is a long-term energy imbalance between the consumption and expenditure of calories. The energy homeostasis is maintained by two kind of hormones; leptin and ghrelin. Leptin suppresses food intake and thereby induces weight loss. Ghrelin, on the other hand, plays a role in meal initiation (Klok, Jakobsdottir, & Drent, 2007)

Imbalance results in leptin resistance

The failure of leptin signaling to suppress food intake and mediate weight loss is commonly referred to as leptin resistance. In this condition, obese individuals do not respond to leptin in an adequate manner (Balland & Cowley, 2015). Thus, high circulating leptin levels are observed in obese human, contrary to theory that absence of

leptin leads to obesity (Carter, Caron, Richard, & Picard, 2013; Myers, Cowley, & Münzberg, 2008).

Leptin signaling pathway

Leptin, a hormone derived from lep gene, is produced and secreted predominantly from white adipose tissues into the circulation and regulates food intake and energy homeostasis in body (Meister, 2000). The central regulation is mediated through the binding of leptin to its receptor, ObR in central nervous system (CNS) (Roujeau, Jockers, & Dam, 2014). Circulating leptin crosses the blood-brain barrier (BBB) through a receptor-mediated endocytosis mechanism and acts on ObR expressed in distinct regions of brain, including arcuate nucleus (ARC) of the hypothalamus (Crujeiras, Carreira, Cabia, Andrade, Amil, & Casanueva, 2015).

Marine natural products

Ocean, covering more than 70% of the earth's surface, is a rich repository of natural resources. Among the total number of species, 80% are living in the ocean ecosystem and are rapidly evolving as an abundant biomass. Moreover, the marine organisms live in an exigent, competitive and aggressive environment that could have resulted in the production of structurally diverse secondary metabolites. These materials include polysaccharides, polyunsaturated fatty acids (PUFA), algal polyphenols, phytocholesterols, pigments, and peptides. The materials have potentials to improve health condition and reduce the risk of diseases. Before several years, a number of novel compounds have been found from marine organisms and their bioactivities have

extensively been studied. These marine natural products possess antioxidant, antihypertensive, anti-inflammatory, antidiabetogenic, and anti-cancer activity. These studies are basis for the development of marine organisms as healthy and functional food ingredients.

Phlorotannins

Marine organisms are rich sources of structurally diverse bioactive compounds with various biological activities. In particular, brown algae contain a variety of bioactive compounds including phlorotannins, polysaccharides, and pigments. Among them, phlorotannins, polymers of phloroglucinols (1,3,5-trihydroxybenzene), possess a variety of biological activities and potential health benefits such as antioxidant activity (A.-R. Kim, Shin, Lee, Park, Park, Yoon, et al., 2009), anti-diabetic activity (Lee, Kang, Ko, Moon, Jeon, Lee, et al., 2014), (Lee, Kang, Ko, Kang, & Jeon, 2013), antihypertensive effects (Li, Wijesekara, Li, & Kim, 2011), matrix metalloproteinase inhibition effect (M.-M. Kim, Van Ta, Mendis, Rajapakse, Jung, Byun, et al., 2006), and anticancer activity (S. J. Park, Kim, & Jeon, 2012), (Y.-I. Yang, Ahn, Choi, & Choi, 2015). Phlorotannins could have the potential and the possibility to develop new functional foods and pharmaceuticals to improve human health (Li, Wijesekara, Li, & Kim, 2011).

Objectives of the study

In this study, we searched for a prospective leptin substitute among natural marine products, and investigated its anti-obesity effects. To select candidates, from marine-derived natural products affecting the leptin signaling pathway, an *in silico* analysis was

performed using the crystal structure of the leptin receptor (PDB ID: 3V6O). Among the examined natural marine products, octaphloretol A (OPA) derived from *Ishige sinicola*, and pyrogallol-phloroglucinol-6,6-bieckol (PP) derived from *Ecklonia cava*, brown algae found along the coast of Jeju Island, Korea, favorably docked to the leptin receptor. Of the candidates that favorably docked to the leptin receptor, OPA (0.1 µg/mL) stimulated the leptin signaling pathway, including STAT5, in hypothalamic N1 neuron cell line. To investigate the anti-obesity effects of OPA through the leptin signaling pathway, 0.25 mg/kg OPA was orally administrated to C57BL/6J obese mice fed on a high-fat diet for 4 weeks, and the leptin signaling pathway was analyzed in the brain, white adipose tissues, liver, and muscle. C57BL/6J obese mice treated with OPA showed reduced body weight and food intake compared to that observed in control obese mice. Furthermore, OPA stimulated leptin receptors, and activated phospho-STAT5 in the hypothalamic arcuate nucleus (ARC). Moreover, OPA activated leptin signaling in all peripheral tissues including white adipose tissues, liver, and muscle. It also reduced the fat size, hepatic steatosis, and regulated glucose metabolism. These results indicate that OPA, a marine-derived bioactive compound, regulates obesity through the leptin signaling pathway in both appetite control via the central nervous system and energy homeostasis via the peripheral nervous system in obese mice fed on a high-fat diet.

LIST OF FIGURES

Fig. 1-1. Crystal structure of ObR and seaweed list for *in silico* docking analysis.

(A) Crystal structure of ObR (PDB ID 3V6O). (B) 13 kinds of phlorotannins derived from these seaweeds were used for docking to ObR.

Fig. 1-2. Crystal structures of phlorotannins for *in silico* docking analysis.

(A) Phloroglucinol, (B) Triphlorethol A, (C) Eckol, (D) Eckstolonol, (E) Tetrafulhalol A, (F) 7-phloro eckol, (G) 6,6-bieckol, (H) Phlorofucofuroeckol A, (I) Dieckol, (J) 2,7-phloroglucinol-6,6-bieckol, (K) Phrogallol-phloroglucinol-6,6-bieckol, (L) Octaphlorethol A, (M) Diphlorethohydroxycarmalol

Fig. 1-3. Chart of all docking poses of the leptin substitute candidates to ObR by

expressed 2 kinds of docking energy; -CDOCKER interaction energy (kcal/mol) and binding energy (kcal/mol). Octaphlorethol A (OPA) and pyrogallol-phloroglucinol-6,6-bieckol (PP) stably bind to ObR with both high -CDOCKER interaction energy and low binding energy and these compounds were the valuable leptin substitute candidates .

Fig. 1-4. Computational prediction of ObR-OPA complex.

ObR is shown as the grass-green ribbon model, and the active site of ObR is shown as the yellow section. OPA is shown as a grey and red stick model and the binding surface between ObR and OPA is expressed as hydrogen bond (B) 2D diagram of ObR-OPA complex. The amino acids of the active site are displayed as a yellow circle. (C) The stability of the ObR-OPA complex is expressed as two types of energy value: the highest -CDOCKER interaction energy is 66.5385 kcal/mol and the lowest total binding energy is -152.105

kcal/mol.

Fig. 1-5. Computational prediction of ObR-PP complex. ObR is shown as the grass-green ribbon model, and the active site of ObR is shown as the yellow section. PP is shown as a grey and red stick model and the binding surface between ObR and PP is expressed as hydrogen bond (B) 2D diagram of ObR-PP complex. The amino acids of the active site are displayed as a yellow circle. (C) The stability of the ObR-PP complex is expressed as two types of energy value: the highest -CDOCKER interaction energy is 76.9756 kcal/mol and the lowest total binding energy is -136.161 kcal/mol.

Fig. 1-6. Cytotoxicity of OPA in hypothalamic N1 cell line. (A) Cytotoxicity of OPA in hypothalamic N1 cell line of 5×10^3 cells/well. (B) Cytotoxicity of OPA in hypothalamic N1 cell line of 1×10^4 cells/well. Values were significantly different from the control at $**P < 0.05$.

Fig. 1-7. Cytotoxicity of PP in hypothalamic N1 cell line. (A) Cytotoxicity of PP in hypothalamic N1 cell line of 5×10^3 cells/well. (B) Cytotoxicity of PP in hypothalamic N1 cell line of 1×10^4 cells/well. Values were significantly different from the control at $**P < 0.05$.

Fig. 1-8. Leptin signaling molecule changes after two kinds of phlorotannins in hypothalamic N1 cell line.

Fig. 2-1. Food intake of C57BL/6J mice. To investigate the appetite control effect of OPA, the food intake of the OPA treated C57BL/6J obese mice was observed for 24 h. The decrease of food intake was observed in OPA (5 mg/kg) treated obese mice compared to food intake of saline treated mice.

Fig. 2-2. Cresyl violet staining of brain of C57BL/6J mice. Neuron cells placed in

ARC of hypothalamus in brain were stained as violet color. The stain rate of HFD group mice was lighter than that of NFD group mice. The stain rate of HFD/OPA group mice, however, was darker than that of HFD group mice.

Fig. 2-3. Expression of leptin receptor and pJAK2 in brain of C57BL/6J mice. Brain tissues were detected using immunohistochemistry.

Fig. 2-4. Expression of pSTAT3 and pSTAT5 in brain of C57BL/6J mice. Brain tissues were detected using immunohistochemistry.

Fig. 2-5. Expression of mTOR and pERK1/2 in brain of C57BL/6J mice. Brain tissues were detected using immunohistochemistry.

Fig. 2-6. Summary of leptin signal mechanism of OPA in brain of C57BL/6J obese mice. OPA directly regulates appetite signal through phosphorylation of STAT5.

Fig. 3-1. Change of body weight of C57BL/6J obese mice oral administrated with OPA during experimental period. The body weights of three groups were measured once a week during experimental period. The results are expressed as mean \pm SD (n=5).

Fig. 3-2. Blood leptin level of C57BL/6J obese mice oral administrated with OPA. Values were significantly different from the control at $***P < 0.05$

Fig. 3-3. Serum analysis of C57BL/6J obese mice oral administrated with OPA. (A) Total cholesterol (B) Triglyceride (C) GOT (D) GPT levels. Values were significantly different from the control at $**P < 0.05$ and $***P < 0.01$.

Fig. 3-4. Size of adipose tissues of C57BL/6J mice. Adipose tissues were stained using H&E method. (A) Stained tissues (B) Pixel area of fat tissues. Values were significantly different from the control at $**P < 0.05$.

Fig. 3-5. Expression of leptin receptor and pJAK2 in adipose tissues of C57BL/6J

mice. Fat tissues were detected using immunohistochemistry.

Fig. 3-6. Expression of pSTAT3 and pSTAT5 in adipose tissues of C57BL/6J mice.

Fat tissues were detected using immunohistochemistry.

Fig. 3-7. Expression of mTOR and pERK1/2 in adipose tissues of C57BL/6J mice.

Fat tissues were detected using immunohistochemistry.

Fig. 3-8. Mechanism of OPA to leptin signal in adipose tissue of C57BL/6J mice.

OPA directly and indirectly affects adipose tissue metabolism through all molecules related with leptin signal pathway.

Fig. 3-9. Histological change of liver tissues of C57BL/6J mice. (A) Weight of liver tissues (B) Stained tissues. The tissues were stained using H&E method.

Fig. 3-10. Expression of leptin receptor and pJAK2 in liver tissues of C57BL/6J mice. Liver tissues were detected using immunohistochemistry.

Fig. 3-11. Expression of pSTAT3 and pSTAT5 in liver tissues of C57BL/6J mice. Liver tissues were detected using immunohistochemistry.

Fig. 3-12. Expression of mTOR and pERK1/2 in liver tissues of C57BL/6J mice. Liver tissues were detected using immunohistochemistry.

Fig. 3-13. Mechanism of OPA to leptin signal in liver tissue of C57BL/6J mice. OPA directly affects hepatic steatosis through phosphorylation of STAT5.

Fig. 3-14. Histological change of muscle tissues of C57BL/6J mice. Muscle tissues were stained using H&E method.

Fig. 3-15. Expression of leptin receptor and pJAK2 in muscle tissues of C57BL/6J mice. Muscle tissues were detected using immunohistochemistry.

Fig. 3-16. Expression of pSTAT3 and pSTAT5 in muscle tissues of C57BL/6J mice.

Muscle tissues were detected using immunohistochemistry.

Fig. 3-17. Expression of mTOR and pERK1/2 in muscle tissues of C57BL/6J mice.

Muscle tissues were detected using immunohistochemistry.

Fig. 3-18. Mechanism of OPA to leptin signal in muscle tissue of C57BL/6J mice.

OPA directly affects glucose metabolism through phosphorylation of both STAT3 and STAT

Part 1.

**Screening of marine-derived bioactive compounds for leptin
receptor agonist and its validation in *in vitro***

Abstract

In this study, we searched for a prospective leptin substitute among natural marine products, and investigated its anti-obesity effects. To select candidates, from marine-derived natural products affecting the leptin signaling pathway, an *in silico* analysis was performed using the crystal structure of the leptin receptor (PDB ID: 3V6O). Among the examined natural marine products, octaphloretol A (OPA) derived from *Ishige sinicola*, and pyrogallol-phloroglucinol-6,6-bieckol (PP) derived from *Ecklonia cava*, brown algae found along the coast of Jeju Island, Korea, favorably docked to the leptin receptor. Of the candidates that favorably docked to the leptin receptor, OPA (0.1 $\mu\text{g/mL}$) stimulated the leptin signaling pathway, including STAT5, in hypothalamic N1 neuron cell line. These results indicate that OPA, a marine-derived bioactive compound, has a potential to regulate obesity through the leptin signaling pathway.

1. Introduction

In silico is an expression meaning ‘performed on computer’ or ‘via computer simulation’. *In silico* approaches in drug discovery effectively screen the drug candidates, thus the techniques reduce the need for expensive lab work and clinical trials. Therefore, *in silico* study has been widely recognized as a powerful technique for identifying hit molecules (Ferreira, dos Santos, Oliva, & Andricopulo, 2015).

Study of structure-activity relationships (SAR) is an essential tool for drug discovery in *in silico* study. Among the molecular modeling methods, molecular docking is a computational method for placing ligands (often small molecules) into the binding site of target receptor (macromolecular target) using their crystal structures in computational space (Ferreira, dos Santos, Oliva, & Andricopulo, 2015). Docking algorithms and scoring functions are capable of generating structures of the target receptor-ligand complexes and estimating the binding energies/affinities (Yuriev, Holien, & Ramsland, 2015).

Marine organisms are rich sources of structurally diverse bioactive compounds with various biological activities. In particular, brown algae contain a variety of bioactive compounds including phlorotannins, polysaccharides, and pigments. Among them, phlorotannins, polymers of phloroglucinols (1,3,5-trihydroxybenzene), possess a variety of biological activities and potential health benefits such as antioxidant activity (A.-R. Kim, et al., 2009), anti-diabetic activity (Lee, et al., 2014), (Lee, Kang, Ko, Kang, & Jeon, 2013), antihypertensive effects (Li, Wijesekara, Li, & Kim, 2011), matrix metalloproteinase inhibition effect (M.-M. Kim, et al., 2006), and anticancer activity (S.

J. Park, Kim, & Jeon, 2012), (Y.-I. Yang, Ahn, Choi, & Choi, 2015). Phlorotannins could have the potential and the possibility to develop new functional foods and pharmaceuticals to improve human health (Li, Wijesekara, Li, & Kim, 2011).

Overweight and obesity are conditions that results in an abnormal or excessive fat accumulation that might have a negative effect on human health (<http://www.who.int/mediacentre/factsheets/en/>). Recently, obesity is rapidly increasing around the world and that has affected on both gender and age (Sáinz, Barrenetxe, Moreno-Aliaga, & Martínez, 2015). The worldwide prevalence of obesity has more than doubled between 1980 and 2014. According to the WHO report estimated in 2014, more than 1.9 billion adults, aged 18 years and older, were overweight. Among them, over 600 million were found to be obese. By definition, 39% of adults were overweight and 13% of them were obese. Moreover, 42 million children, under the age of 5, were overweight or obese in 2013.

The fundamental cause of obesity and overweight is a long-term energy imbalance between the consumed calories and the expended calories. The energy balance is maintained by two kind of hormones; leptin and ghrelin. Leptin suppresses food intake and thereby induces weight loss. Ghrelin, on the other hand, plays a role in meal initiation (Klok, Jakobsdottir, & Drent, 2007; Zabeau, Peelman, & Tavernier, 2015)

The failure of leptin signaling to suppress food intake and mediate weight loss is commonly called leptin resistance that means obese individuals do not respond to leptin in an adequate manner (Balland & Cowley, 2015). Thus, high circulating leptin levels are observed in obese human, contrary to theory that absence of leptin leads to obesity (Myers, Cowley, & Münzberg, 2008), (Carter, Caron, Richard, & Picard, 2013).

In this study, we looked for a prospective leptin substitute among diverse phlorotannins, natural marine products. To select candidates affecting the leptin signaling pathway from a various phlorotannins, an *in silico* analysis was performed using the crystal structure of the leptin receptor (PDB ID: 3V6O). Moreover, the effect of selected candidates on leptin signaling was verified in hypothalamic N1 neuron cell line.

2. Materials and methods

2.1 *In silico* docking of new inhibitor candidates to proteins

For docking studies, the crystal structure of protein was allocated from Protein Data Bank (PDB, <http://www.pdb.org>) and the docking of the protein-ligand complex, the possibility of binding, the precise location of binding site and the binding mode of ligands were performed using CDOCKER in Accelrys Discovery Studio (DS) 3.5 (Accelrys, Inc). CDOCKER, a CHARMM-based docking algorithm, finds favorable docking mode between small molecules and active sites of enzymes in *in silico* computational simulation. To prepare for the docking procedure, we performed the following steps: (1) conversion of the 2D structure into 3D structure; (2) preparing protein and defining the binding site; and (3) docking ligands using CDOCKER (Kang, Lee, Lee, Ko, Kim, Kim, et al., 2015).

2.2. Molecular docking analysis of candidate compounds on ObR

Docking of the selected compounds to ObR was predicted by simulating the interaction between the compounds and ObR by CDOCKER tool in an *in silico* study. The structure of ObR was allocated from Protein Data Bank (PDB: 3V6O). The structural information of candidate compounds was provided from our previous studies and the structures were drawn by CDOCKER tool (Lee, Kang, Ko, Kang, & Jeon, 2013) (Heo, Hwang, Choi, Han, Kim, & Jeon, 2009; Heo & Jeon, 2009; Wijesinghe & Jeon, 2012). To select the candidates of various marine-derived compounds, two kinds of energy value of relative complexes were compared as following: -CDOCKER

interaction energy (kcal/mol) and binding energy (kcal/mol) and expressed as 2 axis chart. Also, the docking poses of the selected compounds to ObR were expressed as 2D diagram and 3D crystal structure.

2.3. Chemicals and reagents

N1 hypothalamic neuron cells were provided from Functional Cellular Networks Laboratory, Gachon University, Republic of Korea. Dulbecco's modified Eagle's medium (DMEM), fetal bovine serum (FBS), penicillin-streptomycin and trypsin-EDTA were purchased from Gibco™ (Burlington, Ont, Canada). 3-(4,5-Dimethylthiazol-2-yl)-2,5-diphenyltetrazolium bromide (MTT) and dimethyl sulfoxide (DMSO) were purchased from Sigma Inc. (St. Louis, MO). Antibodies including pSTAT3, pSTAT5, pJAK2, mTOR and pERK1/2 were purchased from Cell signaling Technology (Beverly, MA). Antibodies including ObR and b-actin were purchased from Abcam (Cambridge, UK). All other chemicals and reagents were analytical grade.

2.4. Cell culture

N1 hypothalamic neuron cells were maintained at 37°C in an incubator, under a humidified atmosphere containing 5% CO₂. The cells were cultured in DMEM supplemented with 10% heat-inactivated FBS, streptomycin (100 µg/ml), penicillin (100 unit/ml).

2.5. Cytotoxicity

Cells were seeded in a 96 well culture plate at a concentration of 5×10^3 cells/well and

1×10^4 cells/well. At 16 h after seeding, the cells were starved using serum free DMEM for 6 h, and then treated with the each compound. The cells were then incubated for an additional 24 h at 37°C . MTS solution was then added to each well. After 4 h of incubation, the absorbance was measured with an ELISA plate reader at 540 nm.

2.6. Assay for leptin signaling pathway

Cells were seeded in a 60 mm dish at a concentration of 1×10^4 cells/well. At 16 h after seeding, the cells were starved using serum free DMEM for 6 h, and then treated with the each compound. The cells were then incubated for an additional 24 h at 37°C .

2.7. Immunoblotting

To validate leptin signaling pathway key molecules such as ObR, pSTAT3, pSTAT5, pJAK2, mTOR, and pERK1/2, equal amounts of proteins (25 ug protein/lane) were separated by 10% sodium dodecyl sulfate–polyacrylamide gel electrophoresis and transferred to polyvinylidene fluoride (PVDF) membrane using semi-dry (25 voltage, 10 min, ATTO). The PVDF membranes were incubated with 5% skim milk as a blocking solution, followed by proper primary antibodies in blocking solution overnight at 4°C . The membranes were washed with Tris-buffered saline with 0.1% tween 20 (TTBS) three times and incubated with appropriate secondary antibodies for 1h at room temperature. The blotting membranes were developed with enhanced chemiluminescence (ATTO) on LAS-4000 (GE healthcare).

2.8. Statistical analysis

All data were expressed as mean \pm standard deviation (SD) of three determinations. Statistical comparison was performed via a one-way ANOVA followed by Duncan's multiple range test (DMRP). P-values of less than 0.001 ($P < 0.001$) and 0.05 ($P < 0.05$) was considered as significant.

3. Results and discussion

3.1 *in silico* docking of marine-derived bioactive compounds to ObR

Bioactive compounds possess multi-functional activities based on their structural characteristics such as hydrophobicity, charge, microelement binding activity. To explore a leptin substitute among marine-derived products, the biological network dynamics between ObR and these marine-derived products were simulated in computational space. Crystal structure of ObR was allocated from Protein Data Bank (PDB ID: 3V6O). 13 kinds of phlorotannins derived from brown seaweed including *Ishige silicola*, *Sarassum siliquastrum*, *Ecklonia cava*, and *Ishige okamurae* were selected as leptin substitute candidates (Fig. 1-1). The structural information of these phlorotannins was provided from our previous studies and the structures were drawn by CDOCKER tool (Fig. 1-2). All docking poses of the leptin substitute candidates to ObR were expressed as 2 dimensional chart using -CDOCKER interaction energy (kcal/mol) and binding energy (kcal/mol) (Fig. 1-3). Among the leptin substitute candidates, two compound candidates stably bind to ObR with both high -CDOCKER interaction energy and low binding energy; Octaphloretol A (OPA) and pyrogallol-phloroglucinol-6,6-bieckol (PP).

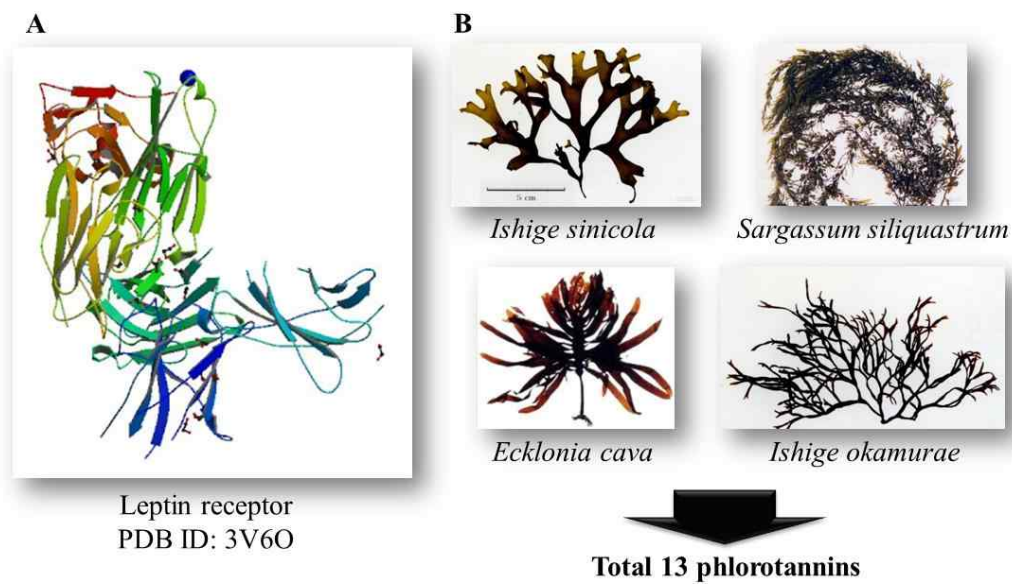


Fig. 1-1. Crystal structure of ObR and seaweed list for in silico docking analysis.
 (A) Crystal structure of ObR (PDB ID 3V6O). (B) 13 kinds of phlorotannins derived from these seaweeds were used for docking to ObR.

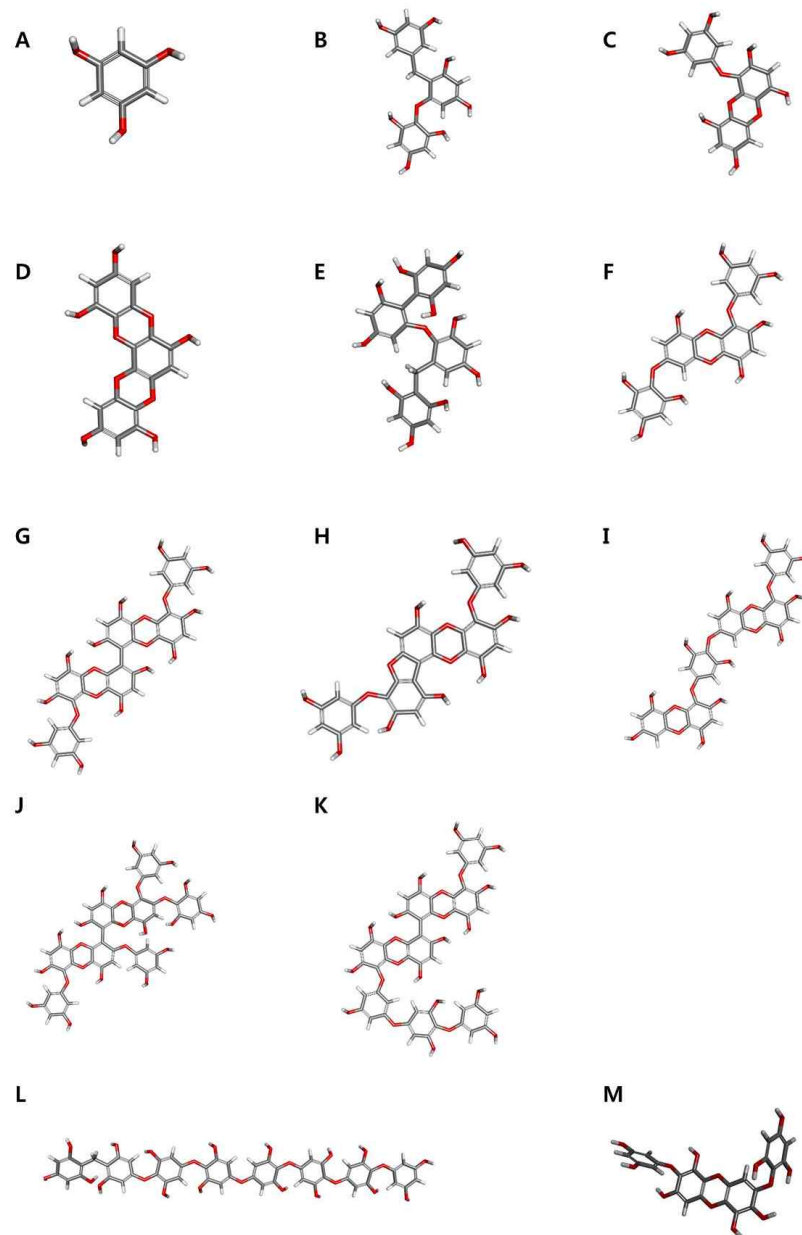


Fig. 1-2. Crystal structures of phlorotannins for *in silico* docking analysis. (A) Phloroglucinol, (B) Triphlorethol A, (C) Eckol, (D) Eckstolonol, (E) Tetrafuhalol A, (F) 7-phloro eckol, (G) 6,6-bieckol, (H) Phlorofucofuroeckol A, (I) Dieckol, (J) 2,7-phloroglucinol-6,6-bieckol, (K) Phrogallol-phloroglucinol-6,6-bieckol, (L) Octaphlorethol A, (M) Diphlorethohydroxycarmalol

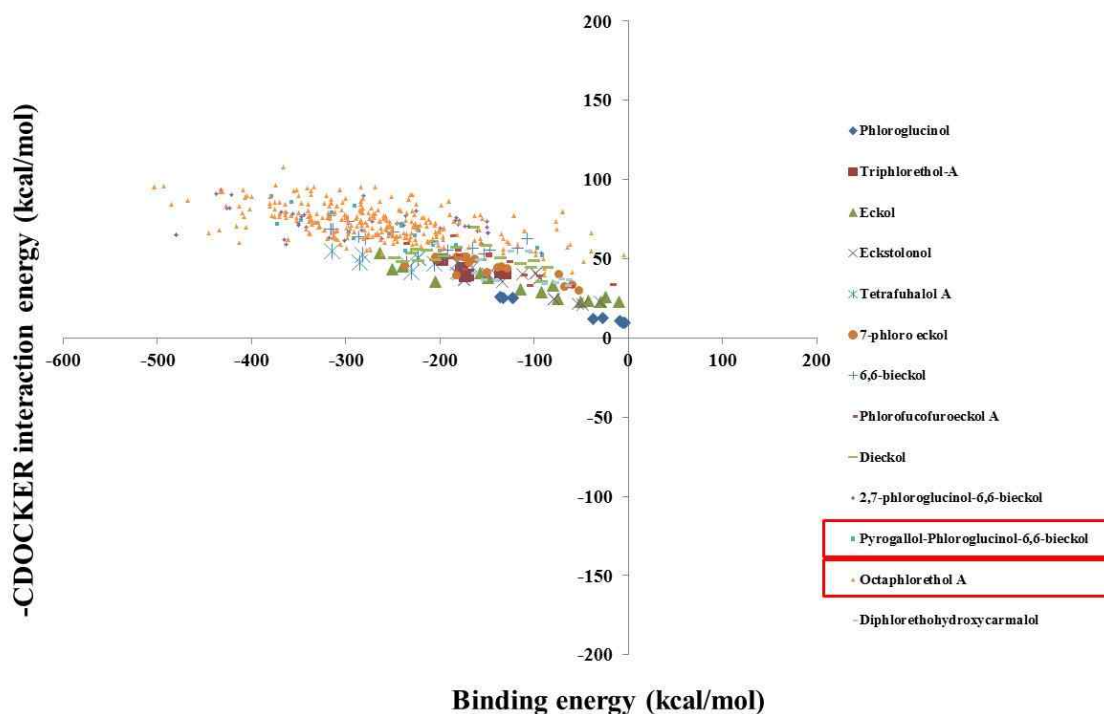


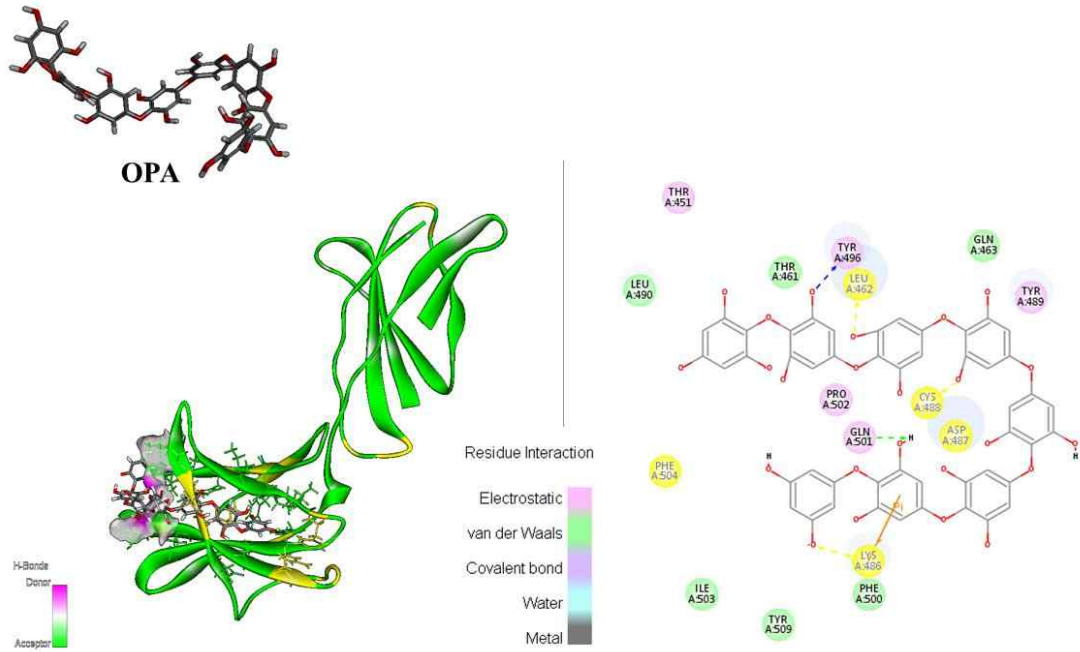
Fig. 1-3. Chart of all docking poses of the leptin substitute candidates to ObR by expressed 2 kinds of docking energy; -CDOCKER interaction energy (kcal/mol) and binding energy (kcal/mol). Octaphloretol A (OPA) and pyrogallol-phloroglucinol-6,6-bieckol (PP) stably bind to ObR with both high -CDOCKER interaction energy and low binding energy and these compounds were the valuable leptin substitute candidates .

3.2 Docking analysis for OPA to ObR

To exactly analyze the biological network dynamics of these docking poses, 2 kinds of selected compounds were analyzed as 3 dimensional docking pose and 2D diagram. The best computational prediction of ObR-OPA complex was shown in Fig. 1-4. The docking of OPA to ObR was performed by interacting with the surface of the enzyme in close proximity to the active site (Fig. 1-4A). ObR was shown as the grass-green ribbon model, and the active site of ObR was shown as the yellow section. OPA was shown as a grey and red stick model and the binding surface between ObR and OPA was expressed as hydrogen bond. ObR-OPA complex displayed the favorable hydrogen bond interaction as the pink section is a donor and the green section is an acceptor (Fig. 1-4A).

The binding position of the ObR-OPA complex was predicted by the 2D diagram (Fig. 1-4B). The docking mode was revealed as a network of hydrogen bond and pi bond following residues: Leu462 (hydrogen bond), Lys486 (hydrogen bond), Lys486 (pi bond), Cys488 (hydrogen bond), Tyr496 (hydrogen bond), Gln501 (Van der Waals bond). Among these amino acids interacting with the part of OPA, three kinds of amino acids, Leu462, Lys486, and Cys488, are main amino acids placed in the active site of ObR. Especially, Lys486 combined with benzene ring of OPA as pi bond.

Moreover, the stability of the ObR-OPA complex was expressed as two types of energy value: the highest -CDOCKER interaction energy was 66.5385 kcal/mol and the lowest total binding energy was -152.105 kcal/mol (Fig. 1-4C).



Binding energy (kcal/mol)	-CDOCKER Energy (kcal/mol)	-CDOCKER Interaction Energy (kcal/mol)
-152.105	26.0054	66.5385

Fig. 1-4. Computational prediction of ObR-OPA complex. ObR is shown as the grass-green ribbon model, and the active site of ObR is shown as the yellow section. OPA is shown as a grey and red stick model and the binding surface between ObR and OPA is expressed as hydrogen bond (B) 2D diagram of ObR-OPA complex. The amino acids of the active site are displayed as a yellow circle. (C) The stability of the ObR-OPA complex is expressed as two types of energy value: the highest -CDOCKER interaction energy is 66.5385 kcal/mol and the lowest total binding energy is -152.105 kcal/mol.

3.3 Docking analysis for PP to ObR

The best computational prediction of PP-OPA complex was shown in Fig. 1-5. The docking of PP to ObR was performed by interacting with the surface of the enzyme in close proximity to the active site (Fig. 1-5A). ObR was shown as the grass-green ribbon model, and the active site of ObR was shown as the yellow section. PP was shown as a grey and red stick model and the binding surface between ObR and PP was expressed as hydrogen bond. ObR-PP complex displayed the favorable hydrogen bond interaction as the pink section is a donor and the green section is an acceptor (Fig. 1-5A).

The binding position of the ObR-PP complex was predicted by the 2D diagram (Fig. 1-5B). The docking mode was revealed as a network of hydrogen bond following residues: Arg468 (hydrogen bond) and Lys486 (hydrogen bond). The amino acids are main amino acids placed in the active site of ObR.

Moreover, the stability of the ObR-PP complex was expressed as two types of energy value: the highest -CDOCKER interaction energy was 76.9756 kcal/mol and the lowest total binding energy was -136.161 kcal/mol (Fig. 1-5C).

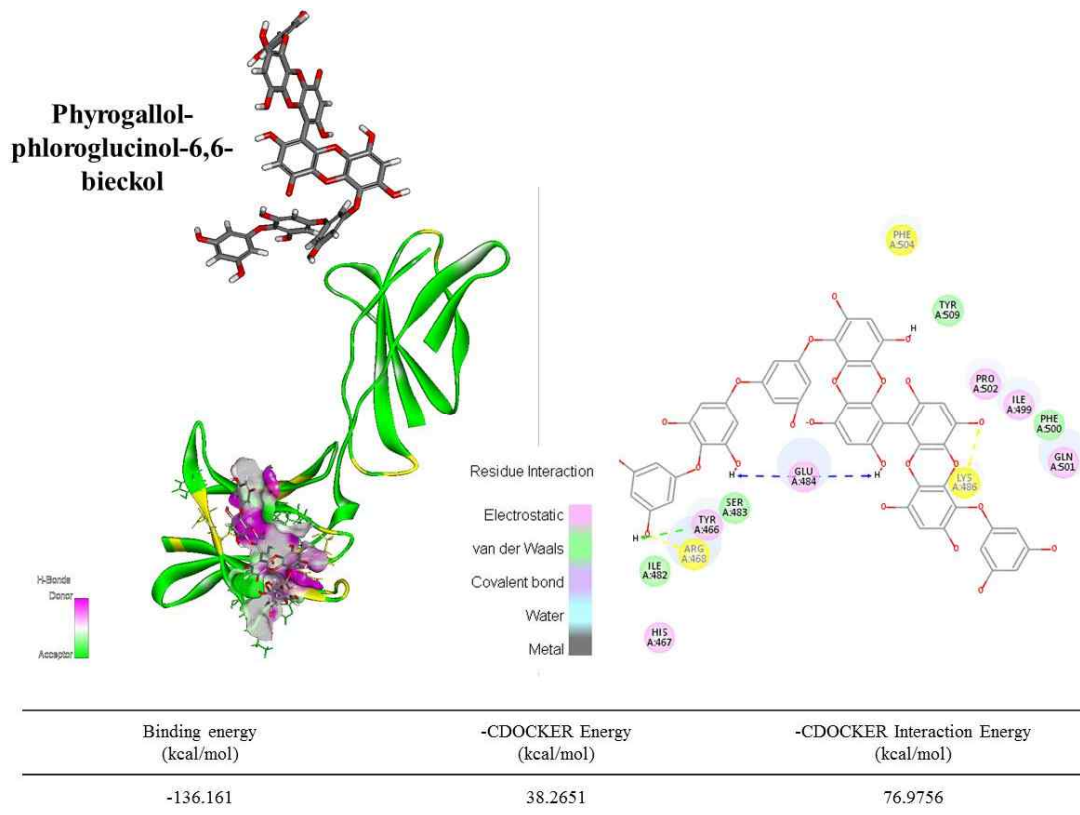
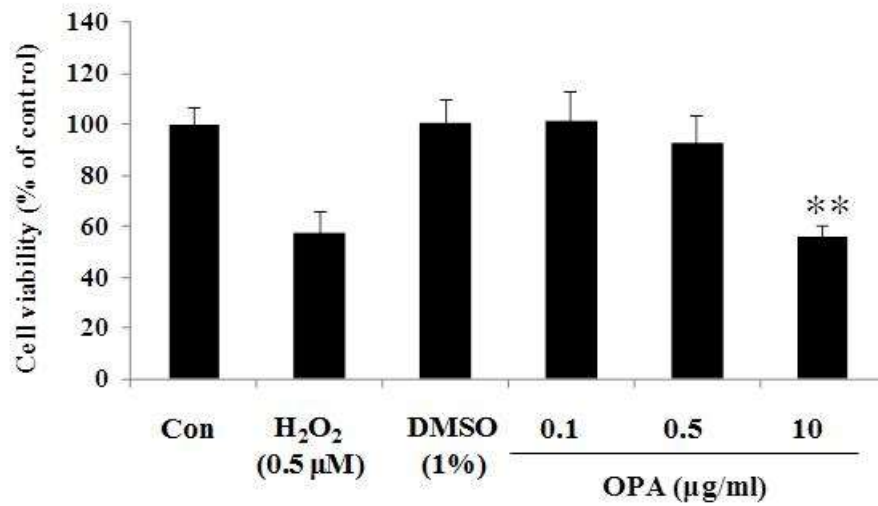


Fig. 1-5. Computational prediction of ObR-PP complex. ObR is shown as the grass-green ribbon model, and the active site of ObR is shown as the yellow section. PP is shown as a grey and red stick model and the binding surface between ObR and PP is expressed as hydrogen bond (B) 2D diagram of ObR-PP complex. The amino acids of the active site are displayed as a yellow circle. (C) The stability of the ObR-PP complex is expressed as two types of energy value: the highest -CDOCKER interaction energy is 76.9756 kcal/mol and the lowest total binding energy is -136.161 kcal/mol.

3.4. Cytotoxicity of the phlorotannins in hypothalamic N1 cell line

We assessed the cytotoxicity of OPA and PP in hypothalamic N1 cells by MTS assay. 0.5 μ M of H₂O₂ was used as positive control and 1% of DMSO was used as solvent for these compounds. Two kinds of number of cells were used for cytotoxicity as following; 5 \times 10³ cells/well and 1 \times 10⁴ cells/well. As shown in Fig. 1-6, OPA showed no cytotoxicity except for the concentrations of 10 μ g/ml on both two kinds of number of cells. Also, PP showed no cytotoxicity in concentration of 12.5 μ g/ml on both two kinds of number of cells (Fig. 1-7). Therefore, we used OPA of 0.25 μ g/ml and PP of 0.5 μ g/ml in the subsequent experiments.

A



B

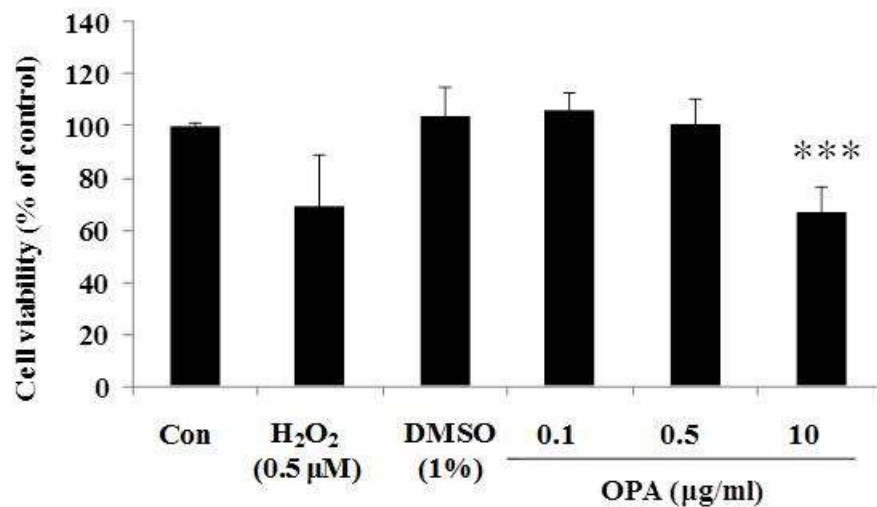
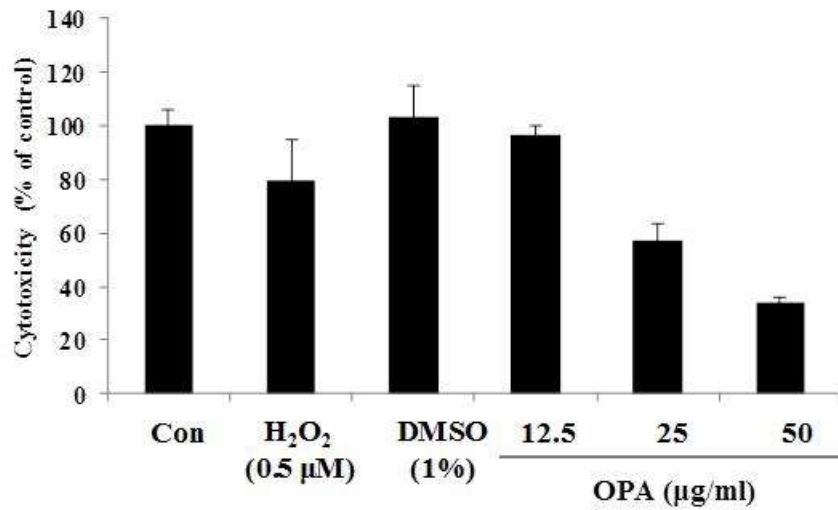


Fig. 1-6. Cytotoxicity of OPA in hypothalamic N1 cell line. (A) Cytotoxicity of OPA in hypothalamic N1 cell line of 5×10^3 cells/well. (B) Cytotoxicity of OPA in hypothalamic N1 cell line of 1×10^4 cells/well. Values were significantly different from the control at $**P < 0.05$.

A



B

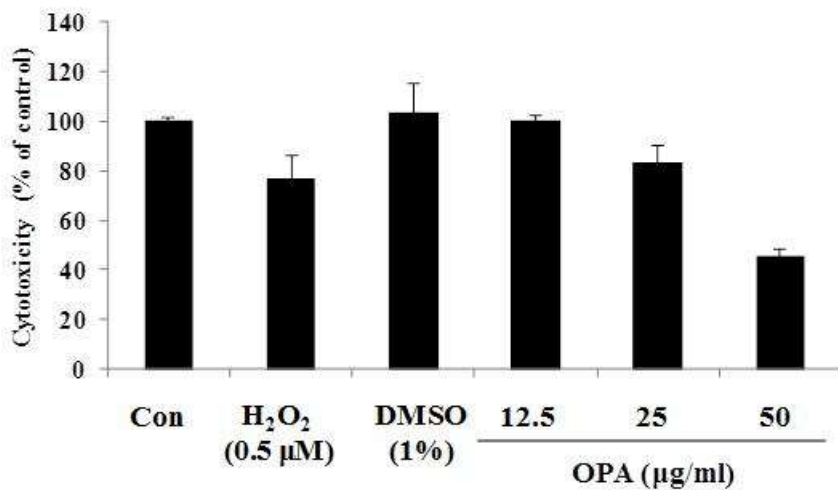


Fig. 1-7. Cytotoxicity of PP in hypothalamic N1 cell line. (A) Cytotoxicity of PP in hypothalamic N1 cell line of 5×10^3 cells/well. (B) Cytotoxicity of PP in hypothalamic N1 cell line of 1×10^4 cells/well. Values were significantly different from the control at $**P < 0.05$.

3.5. Leptin signaling pathway of the phlorotannins in hypothalamic N1 cell line

To investigate the potential mechanism of these compounds, leptin signaling pathway was analyzed after treating these compounds to hypothalamic N1 cells. As shown in Fig. 1-8A, ObR, pSTAT5 and mTOR expression levels in OPA-treated hypothalamic N1 cells were higher than in untreated cells. On the other hand, ObR and pERK1/2 expression levels in PP-treated hypothalamic N1 cells were higher than in untreated cells (Fig. 1-8B). These results showed that OPA and PP have potentials for the appetite control effect through different pathways.

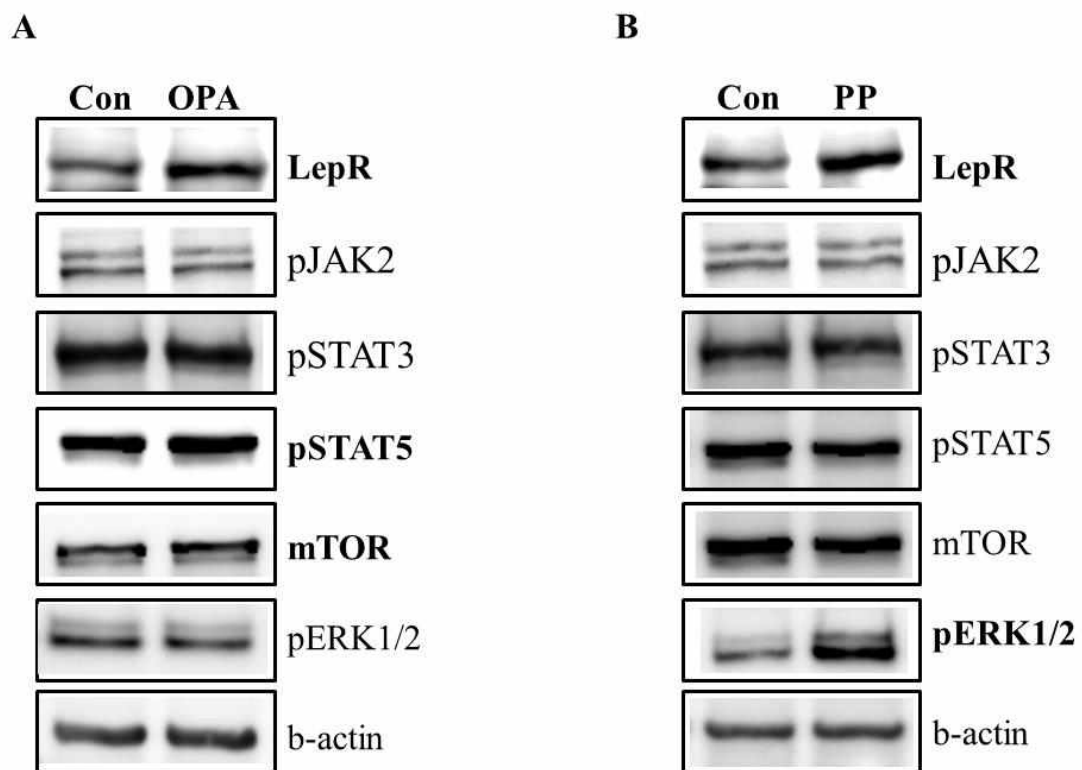


Fig. 1-8. Leptin signaling molecule changes after two kinds of phlorotannins in hypothalamic N1 cell line.

Part 2.

Appetite control effects of octaphlorethol A in central nervous system in obese mice fed with high fat diet

Abstract

To investigate the anti-obesity effects of OPA through the leptin signaling pathway, 0.25 mg/kg OPA was orally administrated to C57BL/6J obese mice fed on a high-fat diet for 4 weeks, and the leptin signaling pathway was analyzed in the brain, white adipose tissues, liver, and muscle. C57BL/6J obese mice treated with OPA showed reduced body weight and food intake compared to that observed in control obese mice. Furthermore, OPA stimulated leptin receptors, and activated phospho-STAT5 in the hypothalamic arcuate nucleus (ARC). These results indicate that OPA, a marine-derived bioactive compound, regulates obesity through the leptin signaling pathway in appetite control via the central nervous system in obese mice fed on a high-fat diet.

1. Introduction

Overweight and obesity are conditions that results in an abnormal or excessive fat accumulation that might have a negative effect on human health (<http://www.who.int/mediacentre/factsheets/en/>). Recently, obesity is rapidly increasing around the world and that has affected on both gender and age (Sáinz, Barrenetxe, Moreno-Aliaga, & Martínez, 2015). The worldwide prevalence of obesity has more than doubled between 1980 and 2014. According to the WHO report estimated in 2014, more than 1.9 billion adults, aged 18 years and older, were overweight. Among them, over 600 million were found to be obese. By definition, 39% of adults were overweight and 13% of them were obese. Moreover, 42 million children, under the age of 5, were overweight or obese in 2013.

The fundamental cause of obesity and overweight is a long-term energy imbalance between the consumed calories and the expended calories. The energy balance is maintained by two kind of hormones; leptin and ghrelin. Leptin suppresses food intake and thereby induces weight loss. Ghrelin, on the other hand, plays a role in meal initiation (Klok, Jakobsdottir, & Drent, 2007). In general, a decreased fat volume in the body (or weight) induces the reduction of the peripheral leptin concentration and increases food intake. Conversely, an increased fat volume in the body induces an increased peripheral leptin concentration and reduced food intake (Sáinz, Barrenetxe, Moreno-Aliaga, & Martínez, 2015).

The failure of leptin signaling to suppress food intake and mediate weight loss is commonly called leptin resistance that means obese individuals do not respond to leptin

in an adequate manner (Balland & Cowley, 2015). Thus, high circulating leptin levels are observed in obese human, contrary to theory that absence of leptin leads to obesity (Myers, Cowley, & Münzberg, 2008), (Carter, Caron, Richard, & Picard, 2013).

Leptin, a hormone derived from *lep* gene, is produced and secreted predominantly from white adipose tissue into the circulation and regulates food intake and energy homeostasis in body. The central regulation is mediated through the binding of leptin to its receptor, ObR in central nervous system (CNS) (Roujeau, Jockers, & Dam, 2014). Circulating leptin crosses the blood-brain barrier (BBB) through a receptor-mediated endocytosis mechanism and acts on ObR expressed in distinct regions of brain, including arcuate nucleus (ARC) of the hypothalamus (Crujeiras, Carreira, Cabia, Andrade, Amil, & Casanueva, 2015).

Ishige sinicola, an edible brown alga, is found throughout the temperate coastal zone of the Korean peninsula. *I. sinicola* generally forms highly persistent populations in clear waters.

Octaphloretol A (OPA) is a phlorotannin isolated from *Ishige sinicola*, and has been reported to possess several biological activities including anti-inflammatory, and antidiabetic effects. Anti-obesity effect of OPA, however, has not been examined (K.-N. Kim, Yang, Kang, Ahn, Roh, Lee, et al., 2015).

In this study, appetite control effects of OPA as leptin substitute were investigated in central nervous system in obese mice fed with high fat diet. To verify the anti-obesity effects of OPA through the leptin signaling pathway, 0.25 mg/kg OPA was orally administrated to C57BL/6J obese mice fed on a high-fat diet for 4 weeks, and the leptin signaling pathway was analyzed in the brain.

2. Materials and methods

2.1. Chemicals and reagents

Antibodies including pSTAT3, pSTAT5, pJAK2, mTOR and pERK1/2 were purchased from Cell signaling Technology (Beverly, MA). Antibodies including ObR and b-actin were purchased from Abcam (Cambridge, UK). All other chemicals and reagents were analytical grade.

2.2. Animals

C57BL/6J mice (5 weeks old male, specific pathogen-free, 19~22 g body weight) were purchased from Central Lab. Animal Inc. (Seoul, Korea). Animals were acclimated in temperature (24°C) controlled rooms with 12 h light/dark cycle. Mice were randomly divided into three experimental groups (n=5 per group) as following; Normal Fat Diet group (NFD), High Fat Diet group (HFD), OPA (2.5 mg/kg) treated High Fat Diet group (HFD/OPA). NFD mice were fed with a standard laboratory diet and HFD mice were fed with rodent diet with 45 kcal fat. After the obesity inducement of HFD group during 6 weeks, OPA was dissolved in saline at a dose of 2.5 mg/kg body weight and orally administrated every day during 4 weeks. Body weight of mice was measured once a week during 12 weeks. After 12 weeks, these mice were anesthetized and blood samples were collected to determine biochemical parameters. The brains were immediately fixed in 4 % paraformaldehyde, and then transferred to 20% sucrose for preparing the frozen block tissue slide. All experiments were performed in accordance with the experimental animal guidelines of Jeju National University animal center.

2.3. Frozen block tissue slide

The brain tissues immersed in 20% sucrose were produced to frozen blocks by embedding the tissues in OCT compound. The frozen blocks were sectioned at a thickness of 6 μ m and the sections were produced to slide. The procedure was processed in cryostat-microtome controlled the temperature (19°C). The slides were kept in -20°C for next experiment.

2.4. Cresyl violet staining

Each section was stained with cresyl violet. All sections were examined by light microscopy (Olympus D970, Olympus Optical Co., Japan).

2.5. Immunohistochemistry

To improve the antigen-antibody reaction, the brain tissues were incubated in antigen retrieval solution (10 mM sodium citrate, 0.05% tween20, pH 6.0) using a microwave for 2 min, and then cooled with ice for 10 min. The brain tissues were washed with PBS for three times. The brain tissues were incubated in blocking solution with normal horse serum for blocking non-specific binding. The brain tissues were incubated overnight with specific antibodies at 4°C and rinsed with PBS. The brain tissues were incubated with fluorescence-conjugated secondary antibodies for 1 h, and then washed with PBS again. The brain tissues were counterstained by 4'6-diamino-2-phenylindole (DAPI) at room temperature for 5 min. The fluorescence signal was detected by confocal microscopy (LSM710, Carl Zeiss).

2.6. Statistical analysis

All data were expressed as a mean \pm standard deviation (SD) of three determinations. Statistical comparison was performed via a one-way ANOVA followed by Duncan's multiple range test (DMRP). P-values of less than 0.001 ($P < 0.001$) and 0.05 ($P < 0.05$) was considered as significant.

3. Results and discussion

3.1. Food intake

To investigate the appetite control effect of OPA, the food intake of the OPA treated C57BL/6J obese mice was observed for 24h (Fig. 2-1). The decrease of food intake was observed in OPA (5mg/kg) treated obese mice compared to food intake of saline treated mice. Especially, the decrease was clearly observed at the early phase after the administration of OPA.

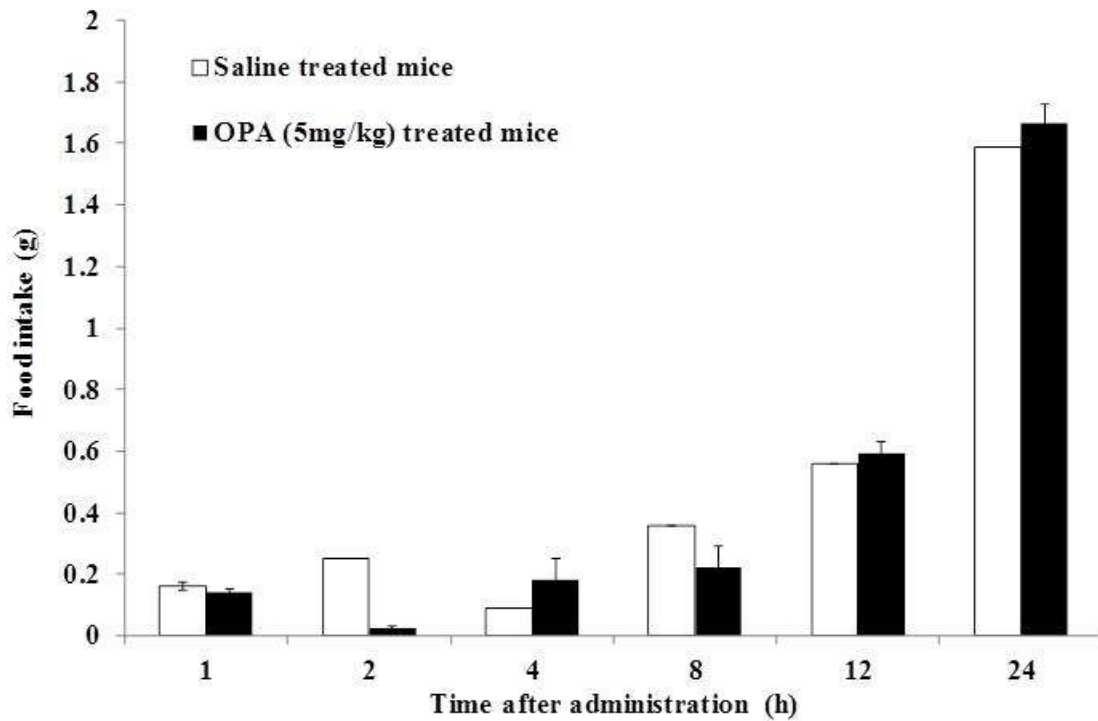


Fig. 2-1. Food intake of C57BL/6J mice. To investigate the appetite control effect of OPA, the food intake of the OPA treated C57BL/6J obese mice was observed for 24 h. The decrease of food intake was observed in OPA (5 mg/kg) treated obese mice compared to food intake of saline treated mice.

3.2. Cresyl violet staining of the brains

Cresyl violet is used to stain Heinz bodies in red blood corpuscles or the neurons in brain and spinal cord. As shown in Fig. 2-2, the brains of C57BL/6J obese mice were stained by cresyl violet. The section of brains is ARC of hypothalamus containing neuropeptide Y (NPY), agouti-related protein (AGRP), and pro-opiomelanocortin (POMC) that is important role in the regulation of appetite (Kamegai, Tamura, Shimizu, Ishii, Sugihara, & Wakabayashi, 2001; Litwak, Wilson, Chen, Garcia-Rudaz, Khaksari, Cowley, et al., 2014). The stain rate of HFD group mice was lighter than that of NFD group mice. The stain rate of HFD/OPA group mice, however, was darker than that of HFD group mice. The result indicated that treatment of OPA recovered the damages of the neuron cells on ARC induced by high fat diet to the NFD group mice levels.

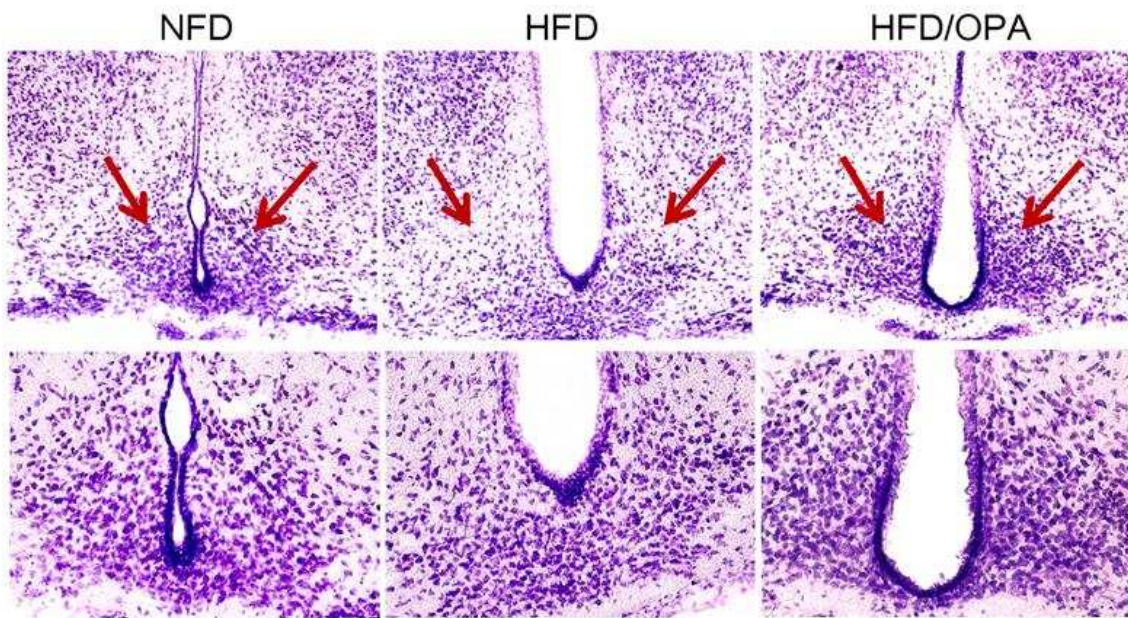


Fig. 2-2. Cresyl violet staining of brain of C57BL/6J mice. Neuron cells placed in ARC of hypothalamus in brain were stained as violet color. The stain rate of HFD group mice was lighter than that of NFD group mice. The stain rate of HFD/OPA group mice, however, was darker than that of HFD group mice.

3.3. Leptin signaling pathway in brain

To identify the effect of OPA on leptin signaling pathway, the expression of key molecules including ObR, pJak2, pSTAT3, pSTAT5, mTOR, and pERK1/2 was confirmed by immunohistochemistry analysis. The expression levels of ObR and pJAK2 were shown in Fig. 2-3. The ObR expression level in brain of HFD group mice was similar with that of NFD mice, however, the level was increased in HFD/OPA group mice at a level of NFD group mice. On the other hand, the pJAK2 expression levels were similar in all of the groups.

The expression levels of pSTAT3 and pSTAT5 were detected to confirm the direct effects of OPA on leptin signaling pathway (Fig. 2-4). The pSTAT3 and pSTAT5 expression level in brain of HFD group mice was significantly decreased compared to that of NFD group mice, however, the level was increased in HFD/OPA group mice above a level of NFD group mice. Especially, pSTAT5 of HFD/OPA group mice was expressed in nucleus of brain.

To confirm the indirect effects of OPA on leptin signaling pathway, the mTOR and pERK1/2 expression levels were detected and shown in Fig. 2-5. The mTOR expression level in brain of HFD group mice was decreased compared to that of NFD group mice, however, the level was increased in HFD/OPA group mice. The pERK1/2 was not expressed in all liver tissues of experimental mice.

In summary, the administration of OPA to C57BL/6J obese mice activated ObR, pSTAT5, and mTOR in brain. Therefore, OPA directly regulated appetite signal through phosphorylation of STAT5.

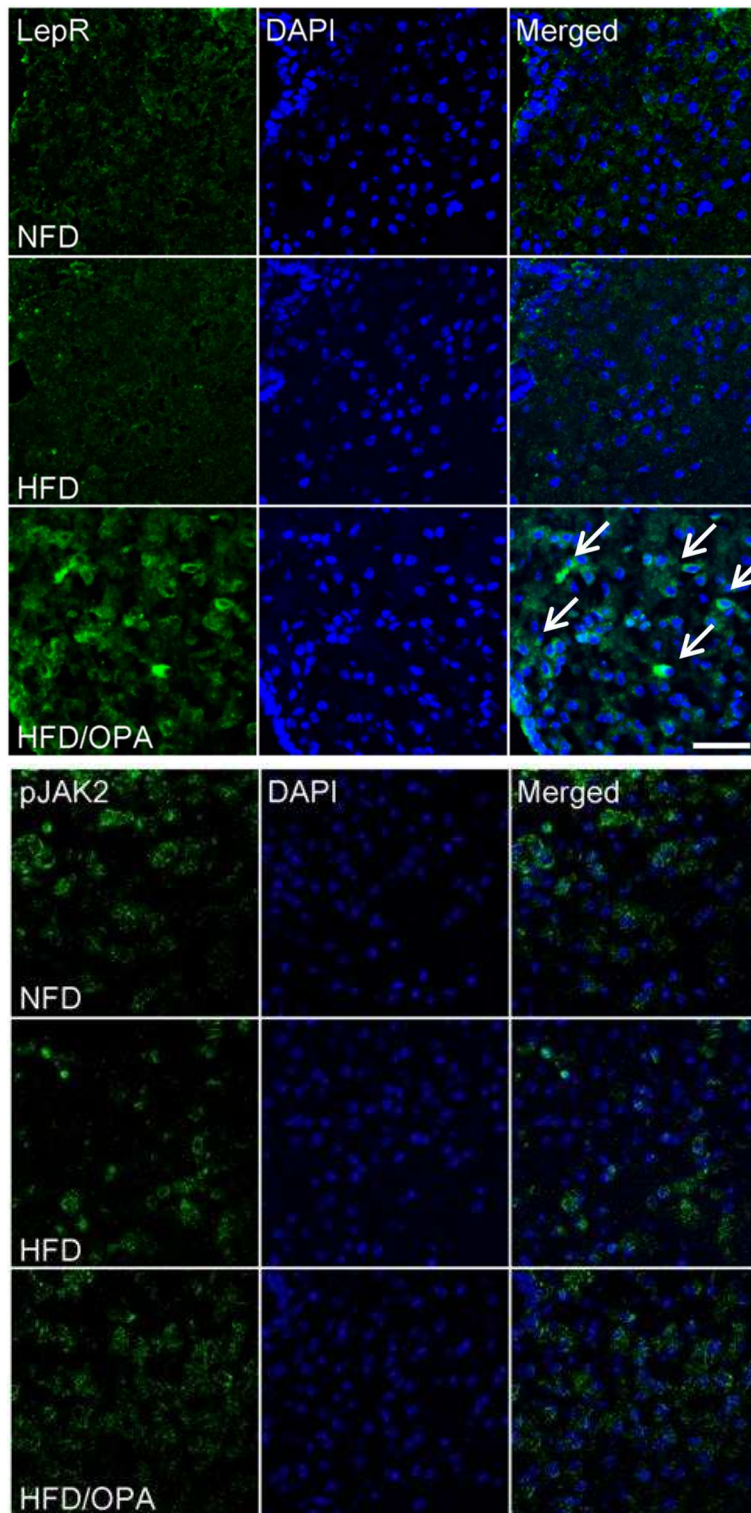


Fig. 2-3. Expression of leptin receptor and pJAK2 in brain of C57BL/6J mice.

Brain tissues were detected using immunohistochemistry.

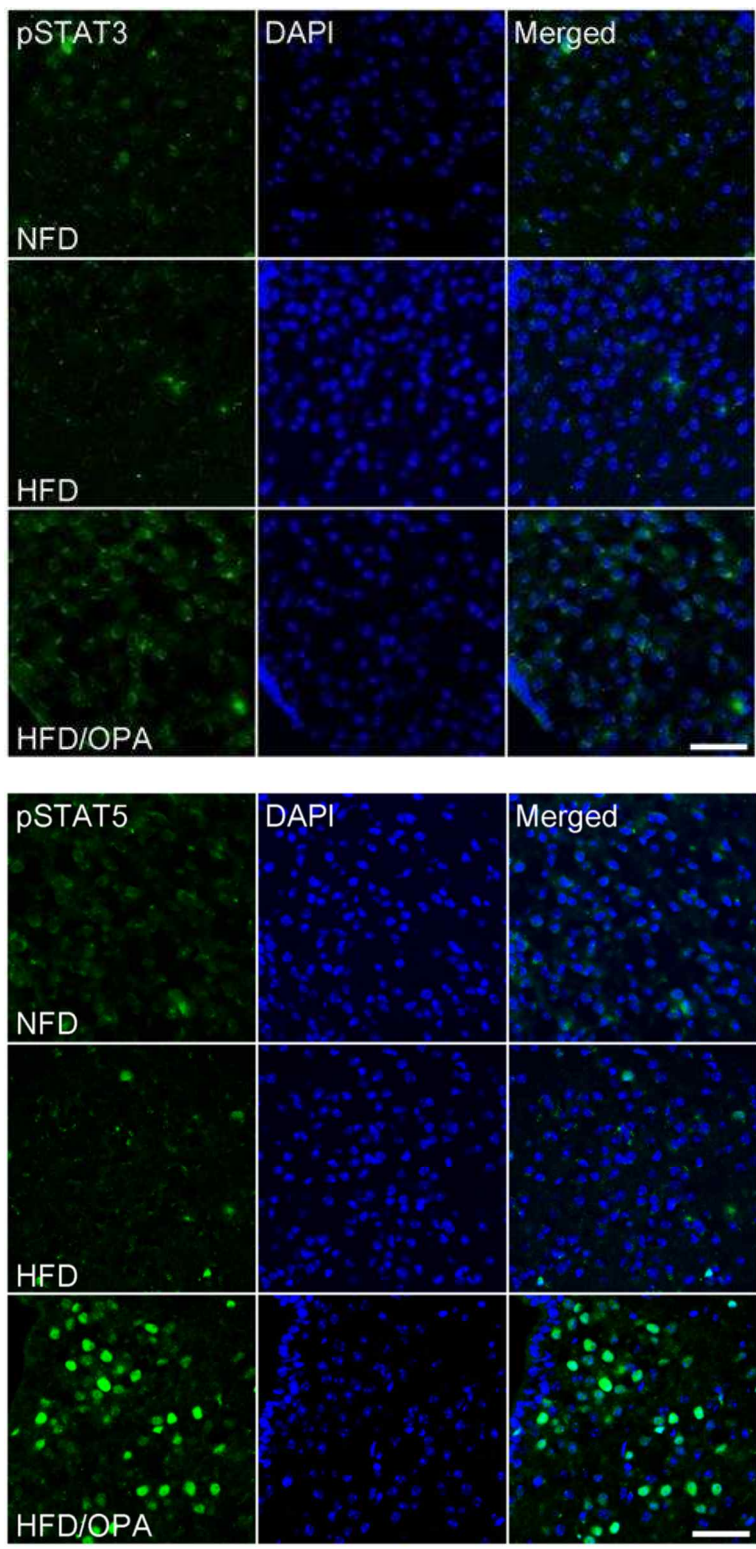


Fig. 2-4. Expression of pSTAT3 and pSTAT5 in brain of C57BL/6J mice. Brain tissues were detected using immunohistochemistry.

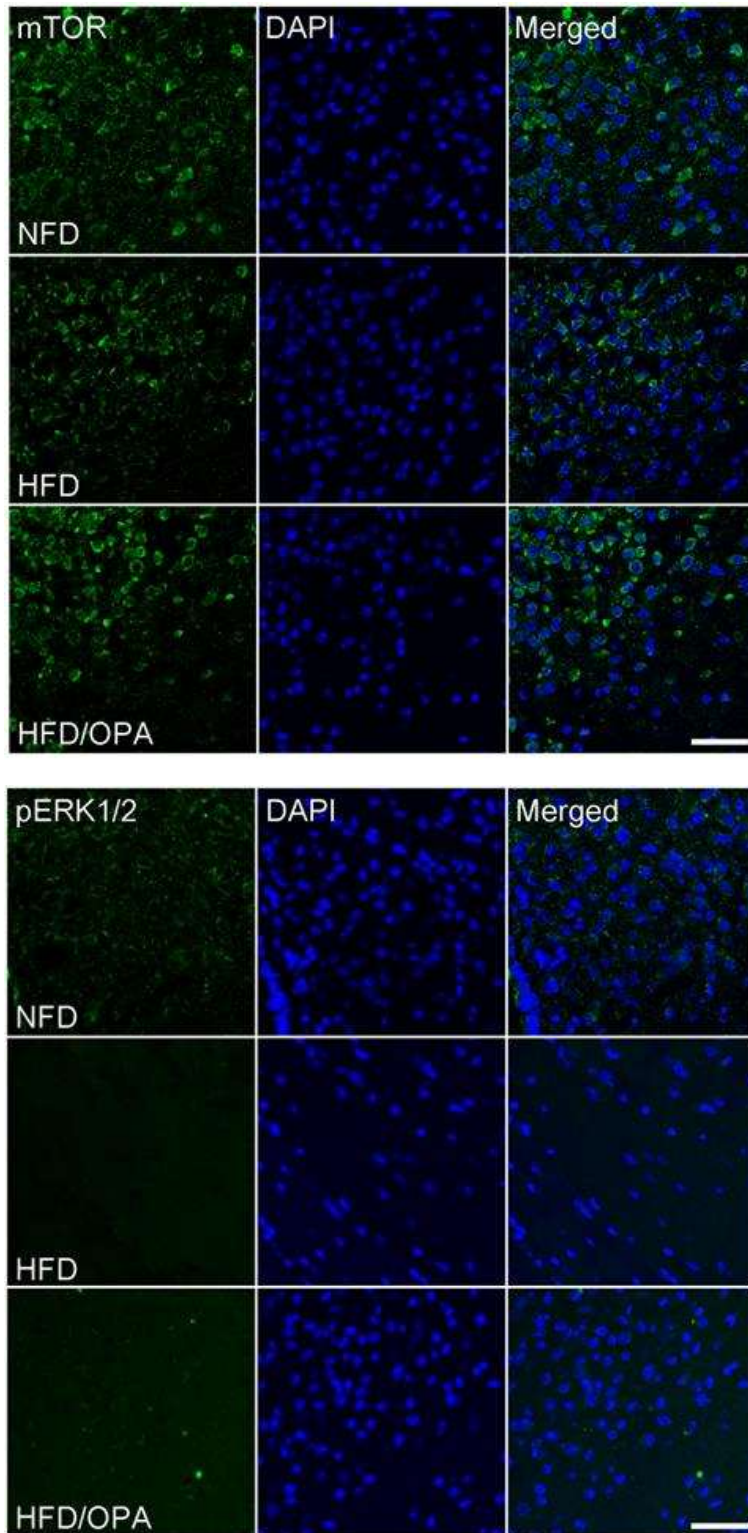


Fig. 2-5. Expression of mTOR and pERK1/2 in brain of C57BL/6J mice. Brain tissues were detected using immunohistochemistry.

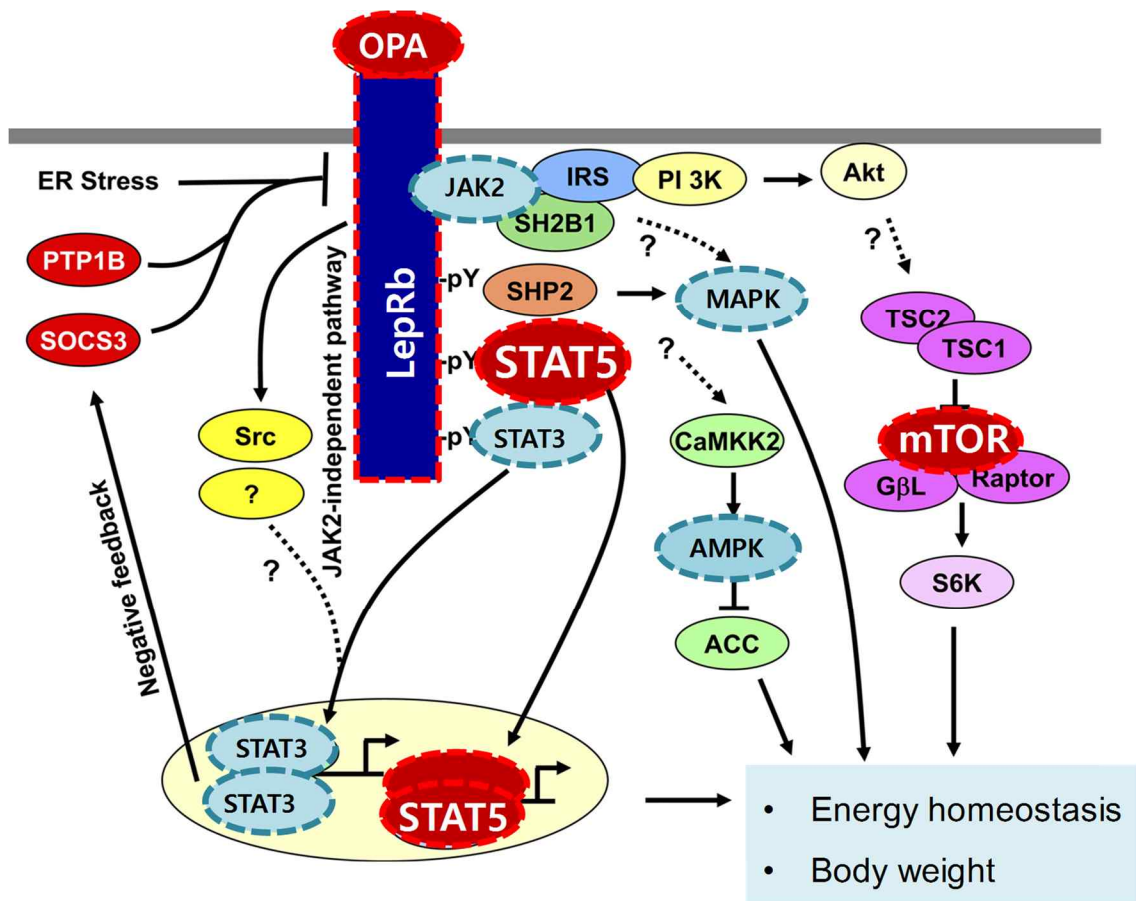


Fig. 2-6. Summary of leptin signal mechanism of OPA in brain of C57BL/6J obese mice. OPA directly regulates appetite signal through phosphorylation of STAT5.

Part 3.

Effects of octaphloretol A on peripheral metabolism as leptin substitute in obese mice fed with high fat diet

Abstract

To investigate the effects of OPA on peripheral metabolism as leptin substitute, 0.25 mg/kg OPA was orally administrated to C57BL/6J obese mice fed on a high-fat diet for 4 weeks, and the leptin signaling pathway was analyzed in white adipose tissues, liver, and muscle. OPA activated leptin signaling in all peripheral tissues. It also reduced the fat size, hepatic steatosis, and regulated glucose metabolism. These results indicate that OPA, a marine-derived bioactive compound, regulates peripheral metabolism through the leptin signaling pathway in obese mice fed with a high-fat diet.

1. Introduction

Leptin, produced from white adipose tissue, is a pleiotropic hormone with a variety of functions in peripheral tissues and organs including adipose tissue, liver, and skeletal muscle (Sáinz, Barrenetxe, Moreno-Aliaga, & Martínez, 2015). Leptin regulates lipolysis, hepatic gluconeogenesis and insulin sensitivity as well as food intake and energy homeostasis and the regulations are more sensitive in obese mice than in its lean littermates (Marti, Berraondo, & Martinez, 1999).

Defects in leptin actions damage lipolytic effect observed in adipocytes by leptin resistance, and it could lead to the development of more and bigger adipocytes and the accumulation of the excessive fat mass (Huynh, Neumann, Wang, Rodrigues, Kieffer, & Covey, 2013). Also, The defects impair the hepatic function leading to hyperglycemia, hyperinsulinemia and hyperlipidemia (Frühbeck, 2002). Leptin resistance, specifically in the liver, modifies the physiological metabolism of lipoproteins and triglycerides. Interestingly, high-fat diet intake alters hepatic gene expression and then induces liver steatosis. Besides, leptin resistance may be involved in the atrophy of skeletal muscle related with obesity and inflammation (Sáinz, Barrenetxe, Moreno-Aliaga, & Martínez, 2015; Sáinz, Rodríguez, Catalán, Becerril, Ramírez, Gomez-Ambrosi, et al., 2010). Thus, leptin deficiency or Peripheral leptin resistance result in obesity, insulin resistance, diabetes, steatosis, inflammation and other features of metabolic syndrome (Chatterjee, Ganini, Tokar, Kumar, Das, Corbett, et al., 2013; Martin, Perez, He, Dawson, & Millard, 2000; H.-K. Park & Ahima, 2015).

In this study, the effects of OPA on peripheral metabolism as leptin substitute were

investigated in obese mice fed with high fat diet. To verify the anti-obesity effects of OPA through the leptin signaling pathway, 0.25 mg/kg OPA was orally administrated to C57BL/6J obese mice fed on a high-fat diet for 4 weeks, and the leptin signaling pathway was analyzed in all peripheral tissues including white adipose tissues, liver, and muscle.

2. Materials and methods

2.1. Chemicals and reagents

Antibodies including pSTAT3, pSTAT5, pJAK2, mTOR and pERK1/2 were purchased from Cell signaling Technology (Beverly, MA). Antibodies including ObR and b-actin were purchased from Abcam (Cambridge, UK). All other chemicals and reagents were analytical grade.

2.2. Animals

C57BL/6J mice (5 weeks old male, specific pathogen-free, 19~22 g body weight) were purchased from Central Lab. Animal Inc. (Seoul, Korea). Animals were acclimated in temperature (24°C) controlled rooms with 12 h light/dark cycle. Mice were randomly divided into three experimental groups (n=5 per group) as following; Normal Fat Diet group (NFD), High Fat Diet group (HFD), OPA (2.5 mg/kg) treated High Fat Diet group (HFD/OPA). NFD mice were fed with a standard laboratory diet and HFD mice were fed with rodent diet with 45 kcal fat. After the obesity inducement of HFD group during 6 weeks, OPA was dissolved in saline at a dose of 2.5 mg/kg body weight and orally administrated every day during 4 weeks. Body weight of mice was measured once a week during 12 weeks. After 12 weeks, these mice were anesthetized and blood samples were collected to determine biochemical parameters. The white adipose tissues and livers were immediately fixed in 4 % paraformaldehyde, and then transferred to 30% sucrose for preparing the paraffin block tissue slide. Also, muscles were immediately fixed in 4 % paraformaldehyde, and then transferred to 20% sucrose for preparing the

frozen block tissue slide. All experiments were performed in accordance with the experimental animal guidelines of Jeju National University animal center.

2.3. Measurement of serum parameters

Serum triglycerides (TGs) and total cholesterol (TC) were analyzed by test kits purchased from Asan Pharm. Co., LTD. (Seoul, Korea). Leptin levels were estimated by an ELISA kit obtained from

2.4. Paraffin block tissue slide

The adipose tissues and liver tissues immersed in 30% sucrose were produced to paraffin blocks by embedding the tissues in paraffin following steps; Tissues were dehydrated by immersing the tissues in ethanol solutions of various concentrations in order of low concentration. After dehydration, tissues were cleared with 100% xylene for 1.5 h, and then embedded in warm paraffin.

2.5. Frozen block tissue slide

The muscles immersed in 20% sucrose were produced to frozen blocks by embedding the tissues in OCT compound. The frozen blocks were sectioned at a thickness of 6 mm and the sections were produced to slide. The procedure was processed in cryostat-microtome controlled the temperature (19°C). The slides were kept in -20°C for next experiment.

2.6. Hematoxylin and eosin staining

The tissue sections were stained with hematoxylin and eosin stain. All sections were examined by light microscopy (Olympus D970, Olympus Optical Co., Japan).

2.7. Immunohistochemistry

To improve the antigen-antibody reaction, the tissue sections were incubated in antigen retrieval solution (10 mM sodium citrate, 0.05% tween20, pH 6.0) using a microwave for 2 min, and then cooled with ice for 10 min. The tissues were washed with PBS for three times. And then, the tissues were incubated in blocking solution with normal horse serum for blocking non-specific binding. The tissues were incubated overnight with specific antibodies at 4°C and rinsed with PBS. The tissues were incubated with fluorescence-conjugated secondary antibodies for 1 h, and then washed with PBS again. The tissues were counterstained by 4'6-diamino-2-phenylindole (DAPI) at room temperature for 5 min. The fluorescence signal was detected by confocal microscopy (LSM710, Carl Zeiss).

2.8. Statistical analysis

All data were expressed as a mean \pm standard deviation (SD) of three determinations. Statistical comparison was performed via a one-way ANOVA followed by Duncan's multiple range test (DMRP). P-values of less than 0.001 ($P < 0.001$) and 0.05 ($P < 0.05$) was considered as significant.

3. Results and discussion

3.1. Changes in body weight of experimental mice

The body weights of three groups were measured once a week during experimental period. As shown in Fig. 3-1, the body weights of all mice were increased compared to initial body weights, however, the difference between three groups was observed at the end of experiment. The body weight of HFD mice was rapidly increased than that of NFD mice, thus, body weight gain of HFD mice was more 8 g higher than that of NFD mice at the end of experiment. The body weight of HFD/OPA mice, however, was relatively lower than that of HFD mice. It indicated that OPA reduced the increasing rate of the body weight induced by high fat diet.

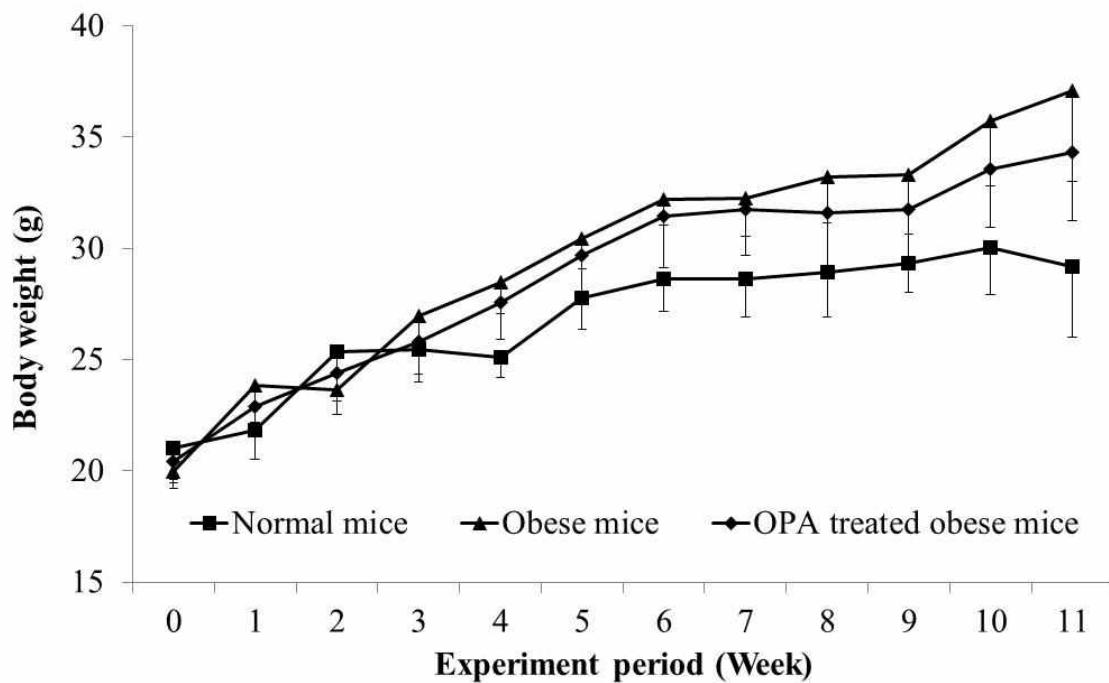


Fig. 3-1. Change of body weight of C57BL/6J obese mice oral administrated with OPA during experimental period. The body weights of three groups were measured once a week during experimental period. The results are expressed as mean \pm SD (n=5).

3.2 Effect of OPA on blood leptin levels

Statistically significant differences between three groups were also observed in various biochemical parameters of carbohydrate and lipid metabolism such as leptin, triglycerides and total cholesterol in serum.

Increased circulating leptin level is a marker of leptin resistance and a common feature in obesity (Miranda, Elias, Hay, Choi, Reed, & Stevens, 2016). The leptin levels of experimental mice are shown in Fig. 3-2. The leptin level of HFD mice was dramatically increased compared to that of NFD mice, and the level is approximately 5 times high value. The leptin level of HFD/OPA mice, however, was relatively lower than that of HFD mice. It indicated that OPA reduced the increasing rate of the circulating leptin level.

Previous studies have shown that plasma leptin levels are elevated in C57BL/6J mice fed high fat diets. These mice fed a normal diet had serum leptin levels below 3 ng/ml but those fed a high fat diet had serum levels of 6 ng/ml or higher (Miranda, Elias, Hay, Choi, Reed, & Stevens, 2016)

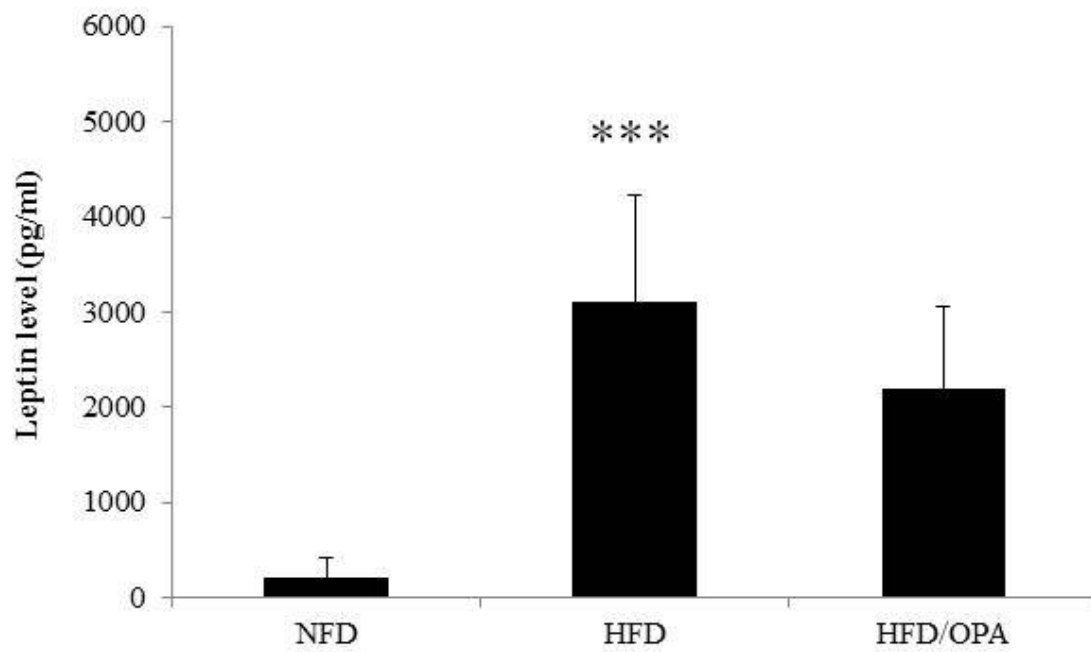


Fig. 3-2. Blood leptin level of C57BL/6J obese mice oral administrated with OPA.

Values were significantly different from the control at ***P < 0.05

3.3. Effect of OPA on serum biochemical levels

We investigated the effects of on the serum levels of total cholesterol and triglyceride in the obese mice (Fig. 3-3). The plasma of total cholesterol and triglyceride levels were significantly increased in the HFD group compared with that in the NFD group, but the levels in HFD/OPA group were relatively decreased compared with that in the HFD group (Fig. 3-3 (A-B)). Moreover, the GOP and GPT levels were significantly increased in the HFD group compared with that in the NFD group, but the levels in HFD/OPA group were relatively decreased compared with that in the HFD group (Fig. 3-3 (C-D)).

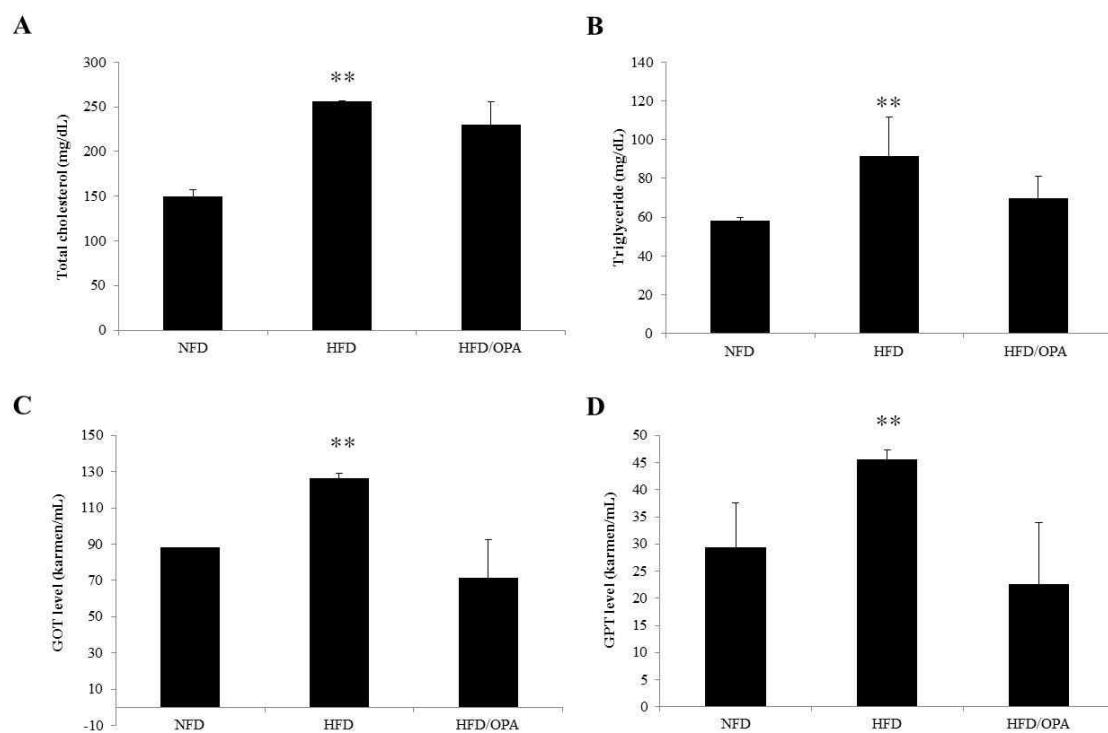


Fig. 3-3. Serum analysis of C57BL/6J obese mice oral administrated with OPA. (A) Total cholesterol (B) Triglyceride (C) GOT (D) GPT levels. Values were significantly different from the control at **P < 0.05 and ***P < 0.01.

3.4. Effect of OPA on adipose tissue metabolism through leptin signaling pathway

Fat accumulation in white adipose tissue was measured using the H&E stain. The morphological changes in the extracted white adipose tissue are shown in Fig. 3-4. The white adipose tissue section of the HFD group showed 2 fold higher increased fat size compared to the section of the NFD group, however, the fat size was decreased in OPA treated HFD group.

To identify the relationship between the changes of fat size and leptin signaling pathway, the expression of key molecules including ObR, pJak2, pSTAT3, pSTAT5, mTOR, and pERK1/2 was confirmed by immunohistochemistry analysis. The expression levels of ObR and pJAK2 were shown in Fig. 3-5. The ObR expression level in adipose tissue of HFD group mice was significantly decreased compared to that of NFD group mice, however, the level was increased in HFD/OPA group mice at a level of NFD group mice. Also, the pJAK2 expression levels were similar with ObR expression levels. The pJAK2 levels in adipose tissue of HFD group mice was significantly decreased compared to that of NFD group mice, however, the level was increased in HFD/OPA group mice.

The expression levels of pSTAT3 and pSTAT5 were detected to confirm the direct effects of OPA on leptin signaling pathway (Fig. 3-6). The pSTAT3 and pSTAT5 expression level in adipose tissue of HFD group mice was significantly decreased compared to that of NFD group mice, however, the level was increased in HFD/OPA group mice above a level of NFD group mice.

To confirm the indirect effects of OPA on leptin signaling pathway, the mTOR and pERK1/2 expression levels were detected and shown in Fig. 3-7. The mTOR and

pERK1/2 expression level in adipose tissue of HFD group mice was significantly decreased compared to that of NFD group mice, however, the level was increased in HFD/OPA group mice at a level of NFD group mice. Especially, the mTOR levels of HFD/OPA group mice was dramatically recovered above a level of NFD group mice

In summary, the administration of OPA to C57BL/6J obese mice activated all of the key molecules, ObR, pJAK2, pSTAT3, pSTAT5, mTOR, and pERK1/2, in the adipose tissue. Therefore, OPA directly and indirectly affects the adipose size through all molecules related with leptin signaling pathway.

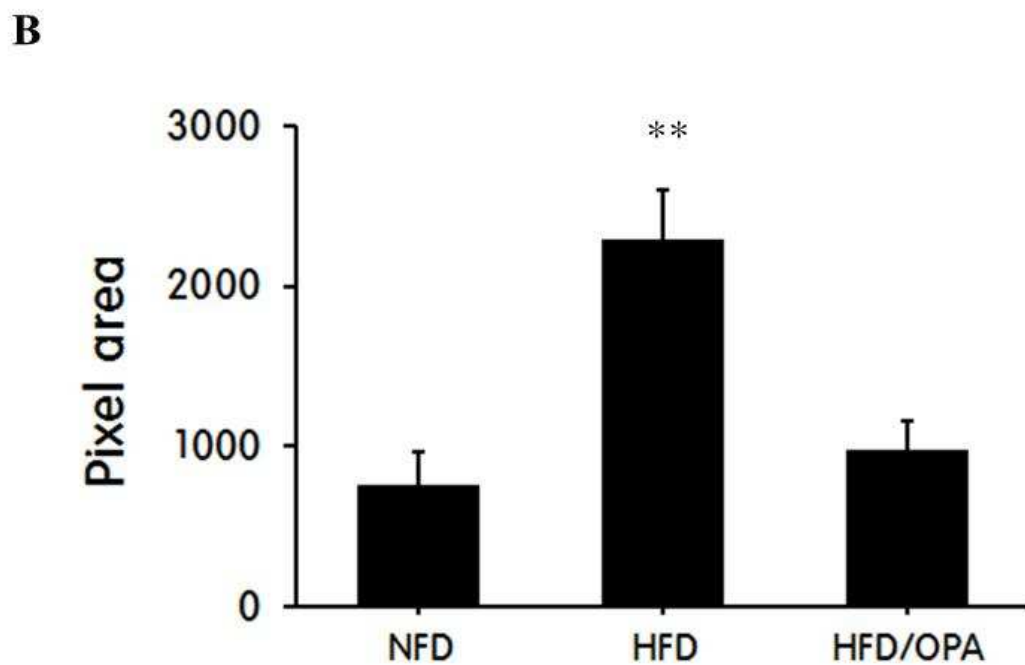
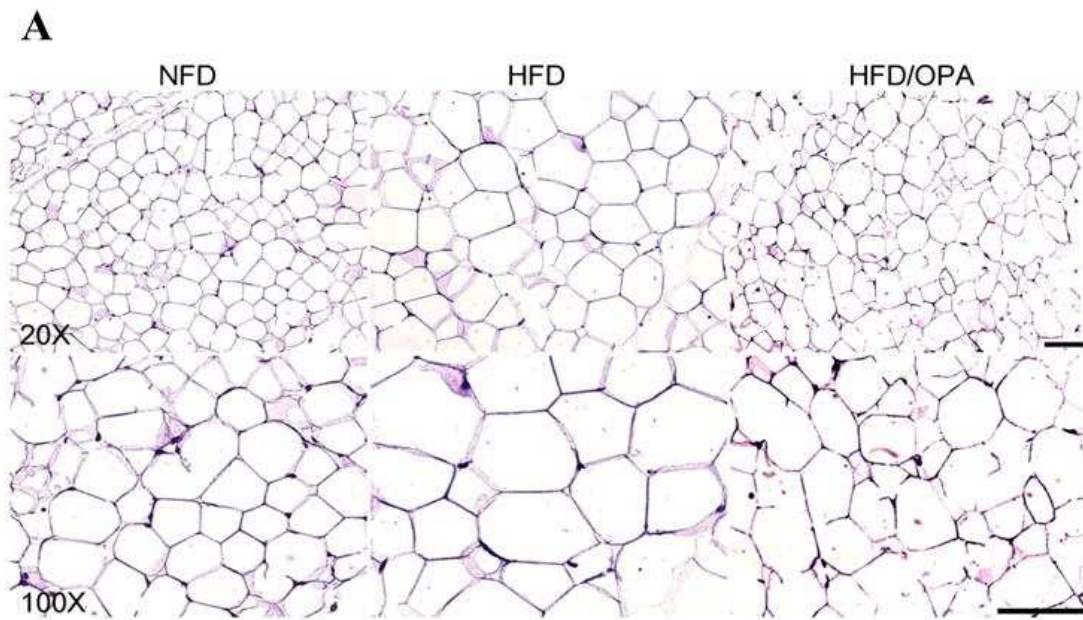


Fig. 3-4. Size of adipose tissues of C57BL/6J mice. Adipose tissues were stained using H&E method. (A) Stained tissues (B) Pixel area of fat tissues. Values were significantly different from the control at $**P < 0.05$.

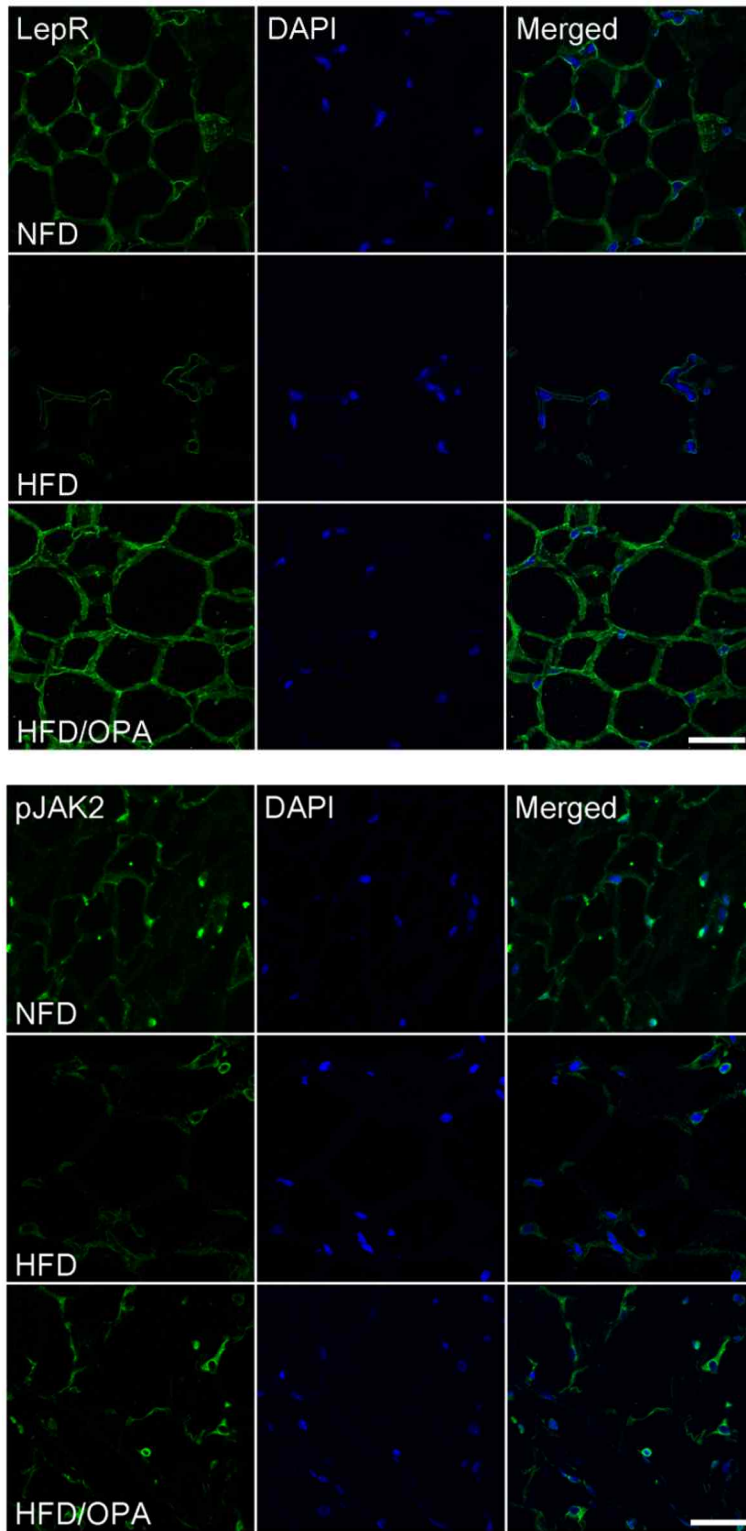


Fig. 3-5. Expression of leptin receptor and pJAK2 in fat tissues of C57BL/6J mice.

Fat tissues were detected using immunohistochemistry.

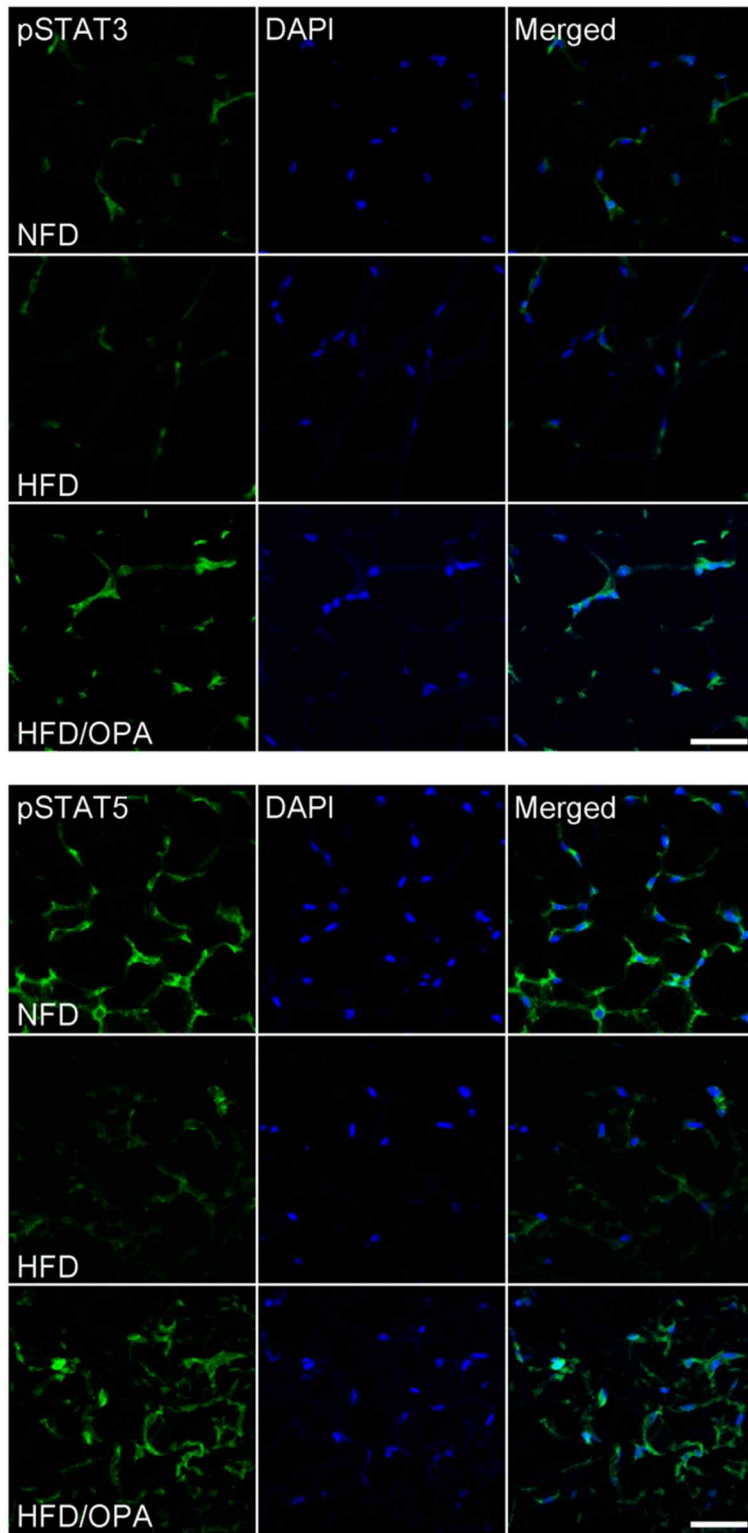


Fig. 3-6. Expression of pSTAT3 and pSTAT5 in fat tissues of C57BL/6J mice. Fat tissues were detected using immunohistochemistry.

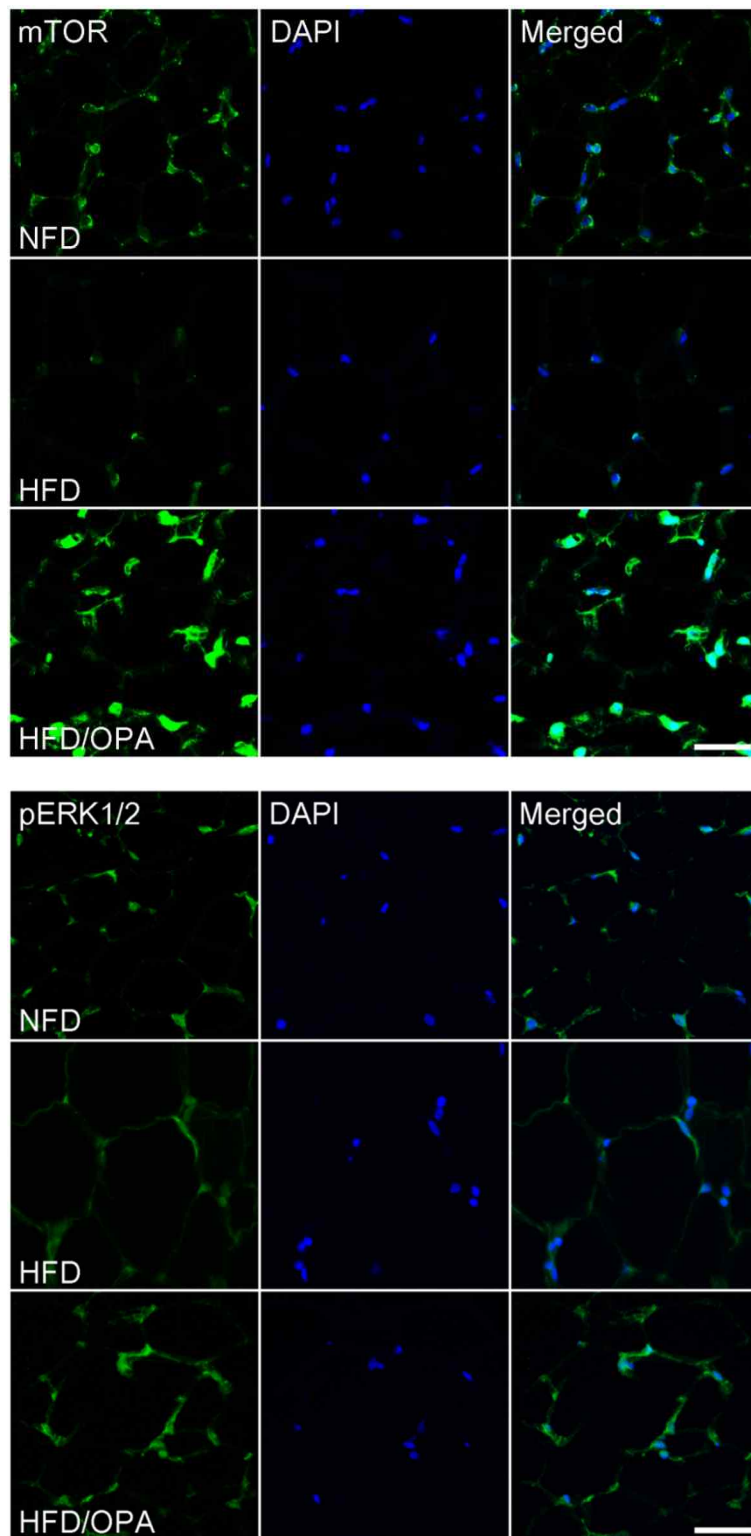


Fig. 3-7. Expression of mTOR and pERK1/2 in fat tissues of C57BL/6J mice. Fat tissues were detected using immunohistochemistry.

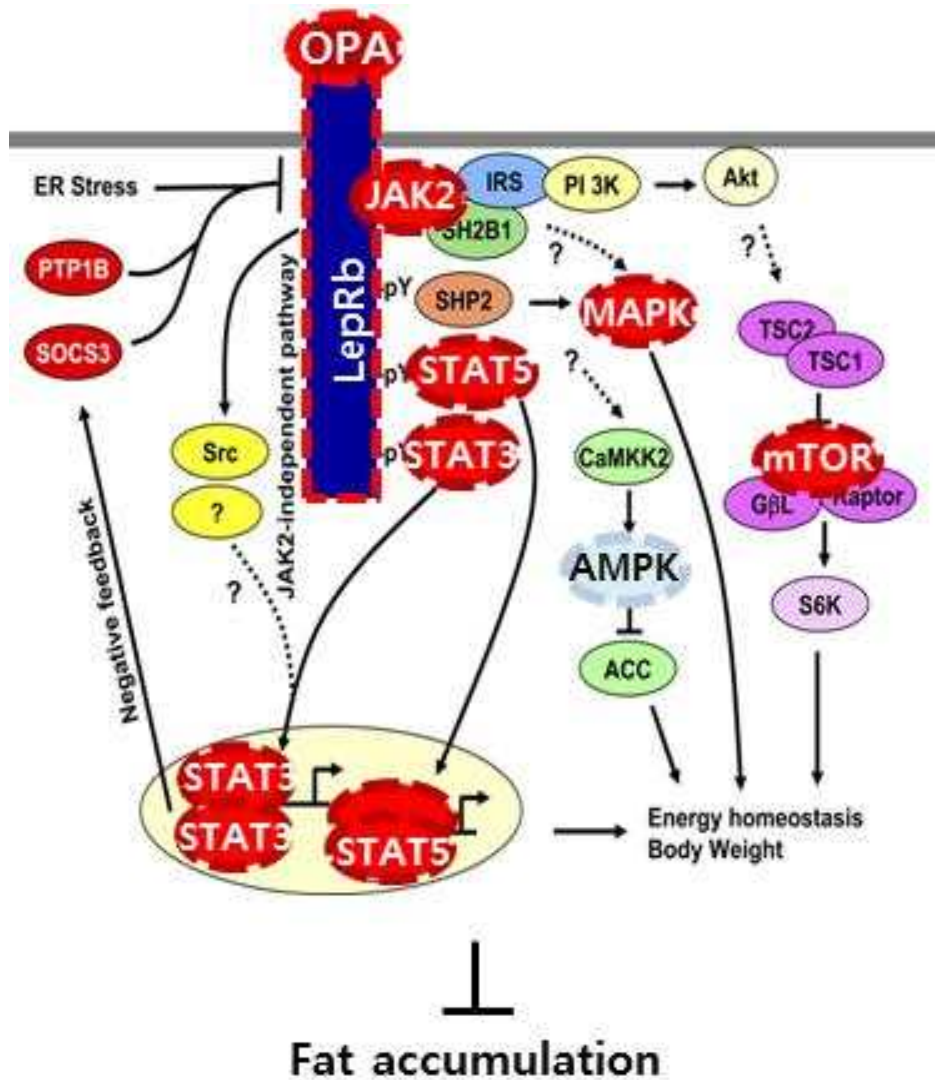


Fig. 3-8. Mechanism of OPA to leptin signal in adipose tissue of C57BL/6J mice.

OPA directly and indirectly affects adipose tissue metabolism through all molecules related with leptin signal pathway.

3.5. Effect of OPA on hepatic steatosis through leptin signaling pathway

Fat accumulation in liver was measured using the H&E stain. The morphological changes in the extracted liver are shown in Fig. 3-12. The liver section of the HFD group showed hepatic steatosis compared with the section of the NFD group, but this was decreased in OPA treated HFD group.

To identify the relationship between the changes of hepatic steatosis and leptin signaling pathway, the expression of key molecules including ObR, pJak2, pSTAT3, pSTAT5, mTOR, and pERK1/2 was confirmed by immunohistochemistry analysis.

The expression levels of ObR and pJAK2 were shown in Fig. 3-10. The ObR expression level in liver of HFD group mice was significantly decreased compared to that of NFD group mice, however, the level was increased in HFD/OPA group mice at a level of NFD group mice. On the other hand, the pJAK2 expression levels were showed as the different pattern with ObR expression levels. The pJAK2 level in liver tissue of HFD group mice was significantly decreased compared to that of NFD group mice. The pJAK2 level of HFD/OPA group mice, however, was not recovered to the level of NFD group mice.

The expression levels of pSTAT3 and pSTAT5 were detected to confirm the direct effects of OPA on leptin signaling pathway (Fig. 3-11). The pSTAT3 and the pSTAT5 expression levels respectively showed the different patterns. The pSTAT3 expression levels were similar in all of the groups. On the other hand, pSTAT5 expression level in liver of HFD group mice was significantly decreased compared to that of NFD group mice, however, the level was increased in HFD/OPA group mice at a level of NFD group mice.

To confirm the indirect effects of OPA on leptin signaling pathway, the mTOR and pERK1/2 expression levels were detected and shown in Fig. 3-12. The mTOR was not expressed in all liver tissues of experimental mice. The pERK1/2 expression level in liver tissue of HFD group mice was significantly decreased compared to that of NFD group mice, however, the level was increased in HFD/OPA group mice at a level of NFD group mice.

In summary, the administration of OPA to C57BL/6J obese mice affected ObR expression. Also, the administration activated pSTAT5 as a direct signal molecule, and pERK1/2 as an indirect signal molecule. pERK1/2, one of the MAPK, signal on leptin signaling pathway is not exactly identified yet. In conclusion, OPA directly affects non-alcoholic steatohepatitis through pSTAT5.

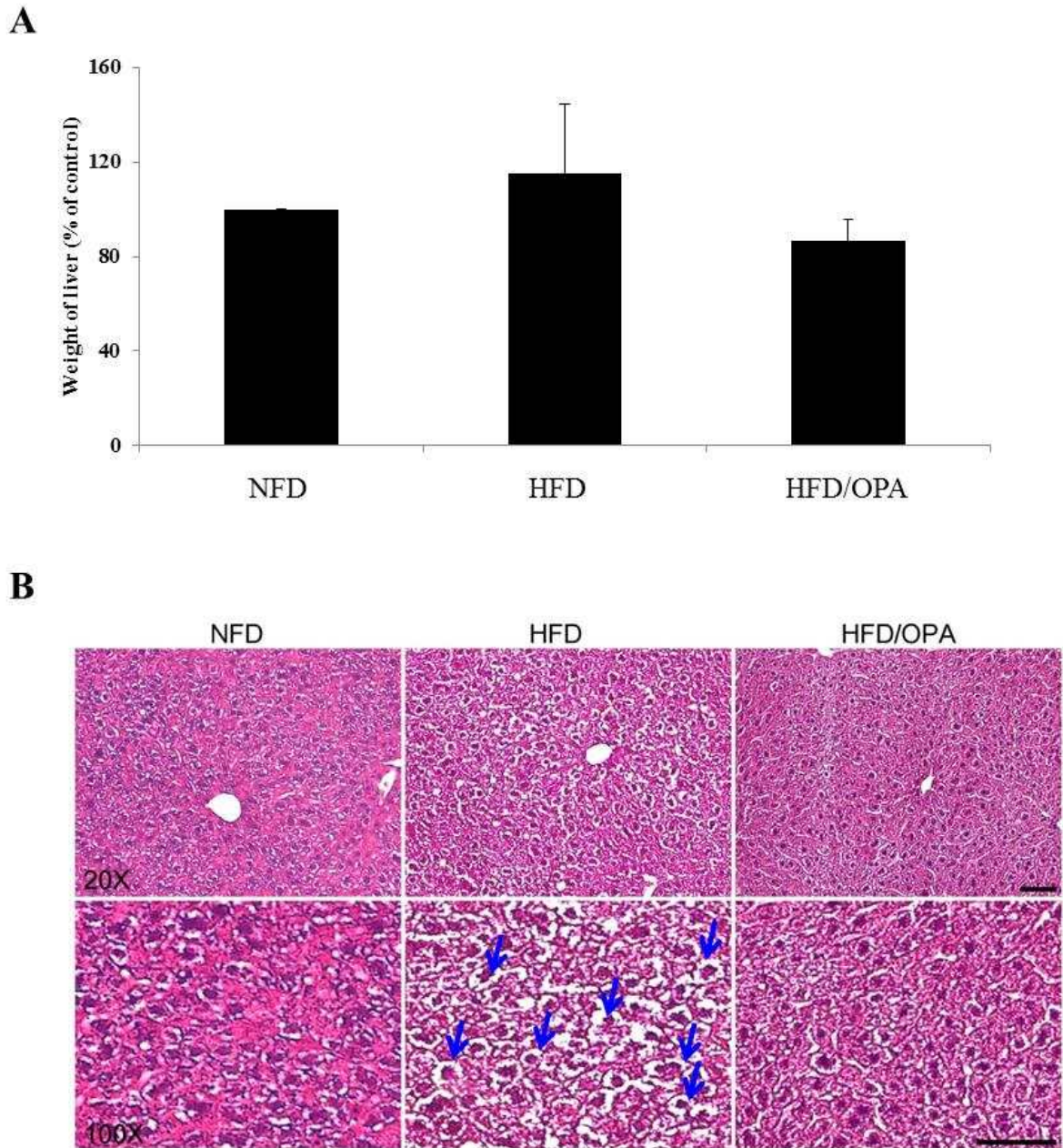


Fig. 3-9. Histological change of liver tissues of C57BL/6J mice. (A) Weight of liver tissues (B) Stained tissues. The tissues were stained using H&E method.

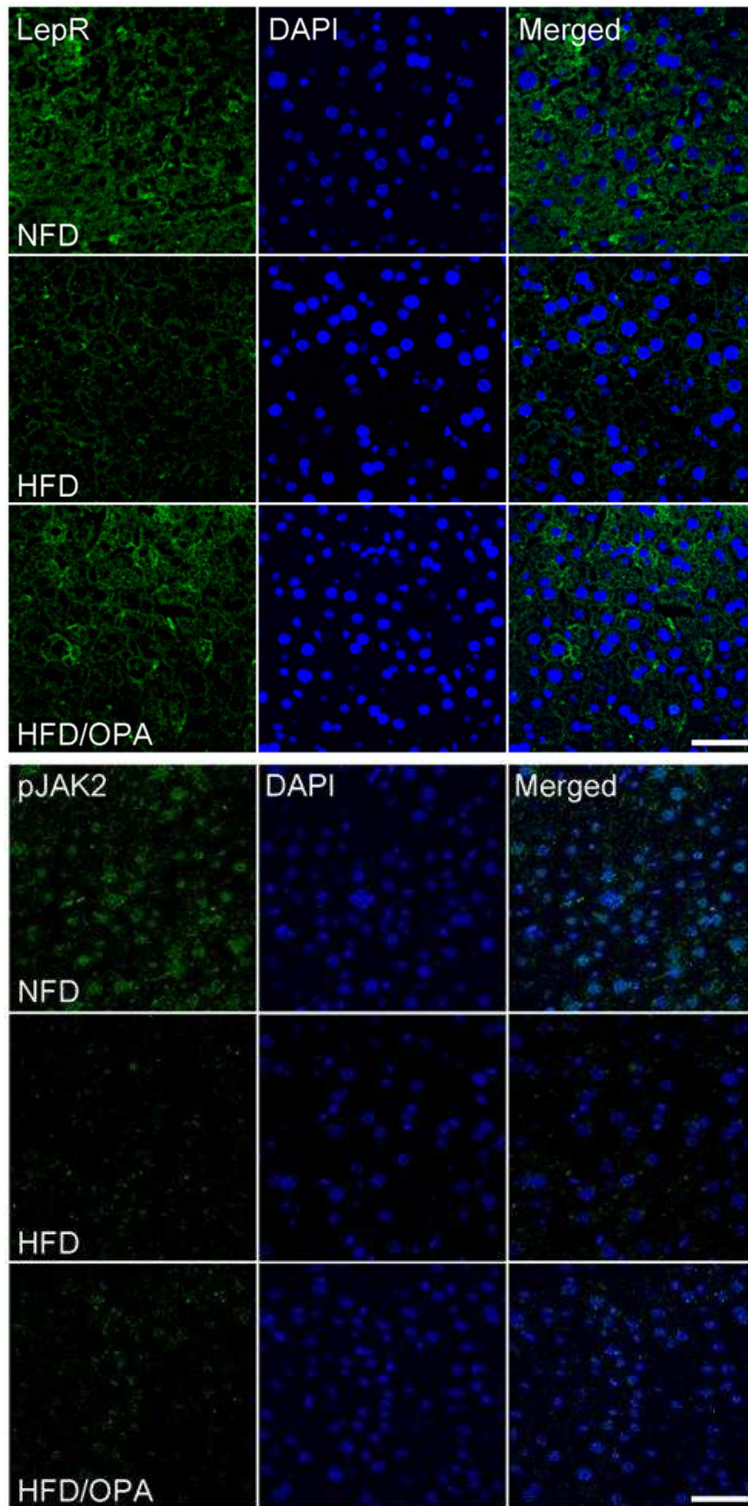


Fig. 3-10. Expression of leptin receptor in liver tissues of C57BL/6J mice. Liver tissues were detected using immunohistochemistry.

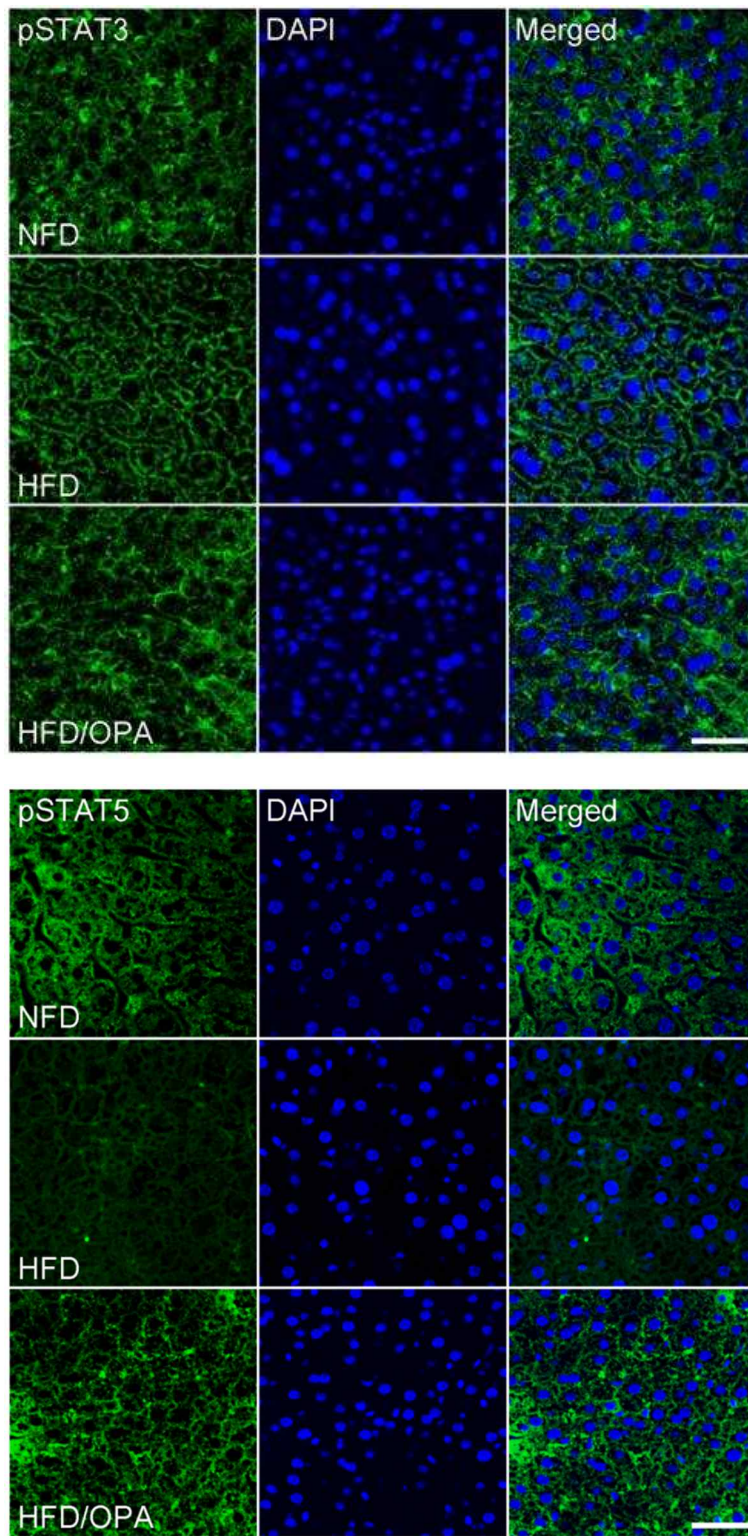


Fig. 3-11. Expression of pSTAT3 and pSTAT5 in liver tissues of C57BL/6J mice.

Liver tissues were detected using immunohistochemistry.

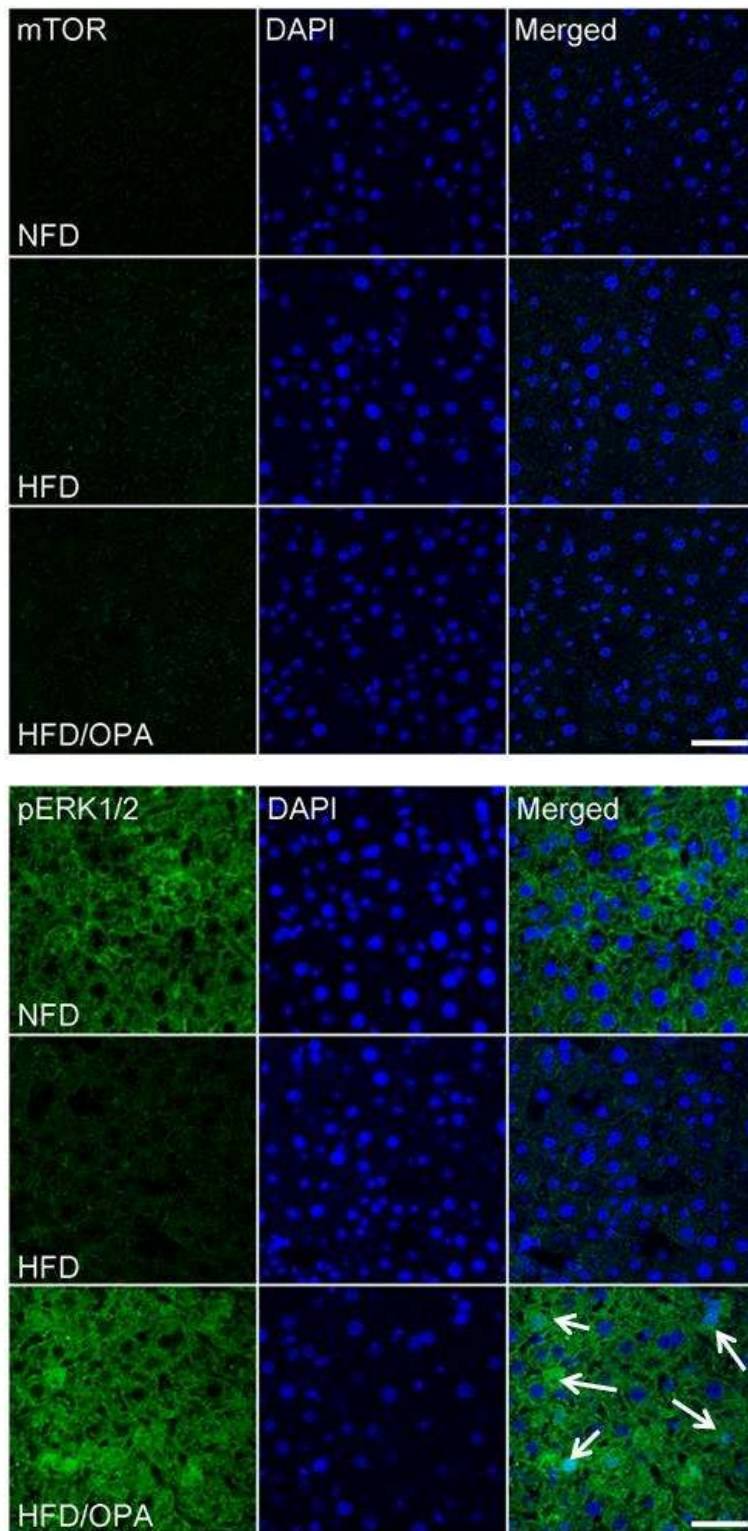


Fig. 3-12. Expression of mTOR in liver tissues of C57BL/6J mice. Liver tissues were detected using immunohistochemistry.

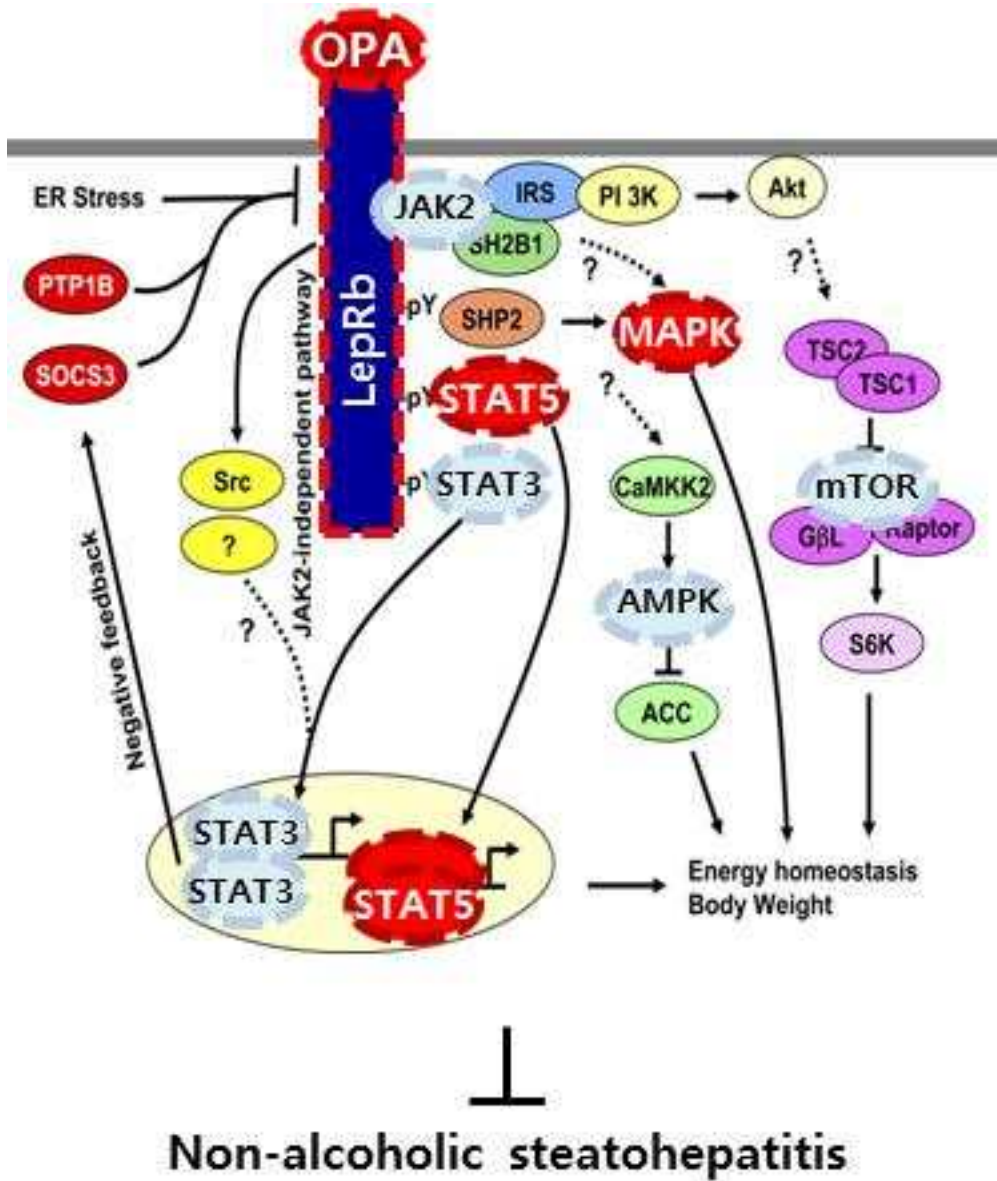


Fig. 3-13. Mechanism of OPA to leptin signal in liver tissue of C57BL/6J mice.

OPA directly affects hepatic steatosis through phosphorylation of STAT5.

3.6. Effect of OPA on glucose metabolism through leptin signaling pathway

Fat accumulation in muscle was measured using the H&E stain. The morphological changes in the extracted muscle are shown in Fig. 3-20. The muscle section of the HFD group showed steatosis compared with the section of the NFD group, but this was decreased in OPA treated HFD group.

To identify the relationship between the changes of steatosis and leptin signaling pathway, the expression of key molecules including ObR, pJak2, pSTAT3, pSTAT5, mTOR, and pERK1/2 was confirmed by immunohistochemistry analysis.

The expression levels of ObR and pJAK2 were shown in Fig. 3-15. The ObR expression level in muscle tissue of HFD group mice was significantly decreased compared to that of NFD group mice, however, the level was increased in HFD/OPA group mice at a level of NFD group mice. On the other hand, the pJAK2 expression levels were similar in all of the groups.

The expression levels of pSTAT3 and pSTAT5 were detected to confirm the direct effects of OPA on leptin signaling pathway (Fig. 3-16). The pSTAT3 and pSTAT5 expression level in muscle tissue of HFD group mice was significantly decreased compared to that of NFD group mice, however, the level was increased in HFD/OPA group mice above a level of NFD group mice.

To confirm the indirect effects of OPA on leptin signaling pathway, the mTOR and pERK1/2 expression levels were detected and shown in Fig. 3-17. The mTOR level of HFD/OPA group mice was not recovered to the level of NFD group mice. On the other hand, The pERK1/2 expression level in muscle tissue of HFD group mice was significantly decreased compared to that of NFD group mice, however, the level was

increased in HFD/OPA group mice at a level of NFD group mice.

In summary, the administration of OPA to C57BL/6J obese mice affected ObR expression. Also, the administration activated both pSTAT3 and pSTAT5 as direct signal molecules, and pERK1/2 as an indirect signal molecule. pERK1/2, one of the MAPK, signal on leptin signaling pathway is not exactly identified yet. In conclusion, OPA directly affects steatosis through phosphorylation of both STAT3 and STAT5.

Peripherally, leptin is implicated in a broad range of physiological processes such as angiogenesis, hematopoiesis, bone formation, wound healing, immunocompetence or lipid and carbohydrate metabolism regulation and nutrient intestinal absorption (Sáinz, Barrenetxe, Moreno-Aliaga, & Martínez, 2015).

The mice model of high fat diet has been widely used to investigate anti-obesity effects and the development of anti-obesity medications. Obesity resulting from overeating causes a dyslipidemia-associated metabolic disorder. The high fat diet-induced obesity in mice is characterized by increased adipocyte size, body weight, and fatty liver. In particular, triglyceride and cholesterol levels are closely related to cardiovascular disorders. Previously reported studies have shown that obese mice induced by high fat diet exhibited characteristics of metabolic disorders, such as hyperlipidemia and hypercholesteremia (Litwak, et al., 2014).

Our results indicate that OPA improved high fat diet-induced body weight, adipose size, fatty liver, total cholesterol and triglyceride levels. In conclusion, these data suggest that OPA has potent anti-obesity activity, therefore, could be developed as a therapeutic agent for obesity.

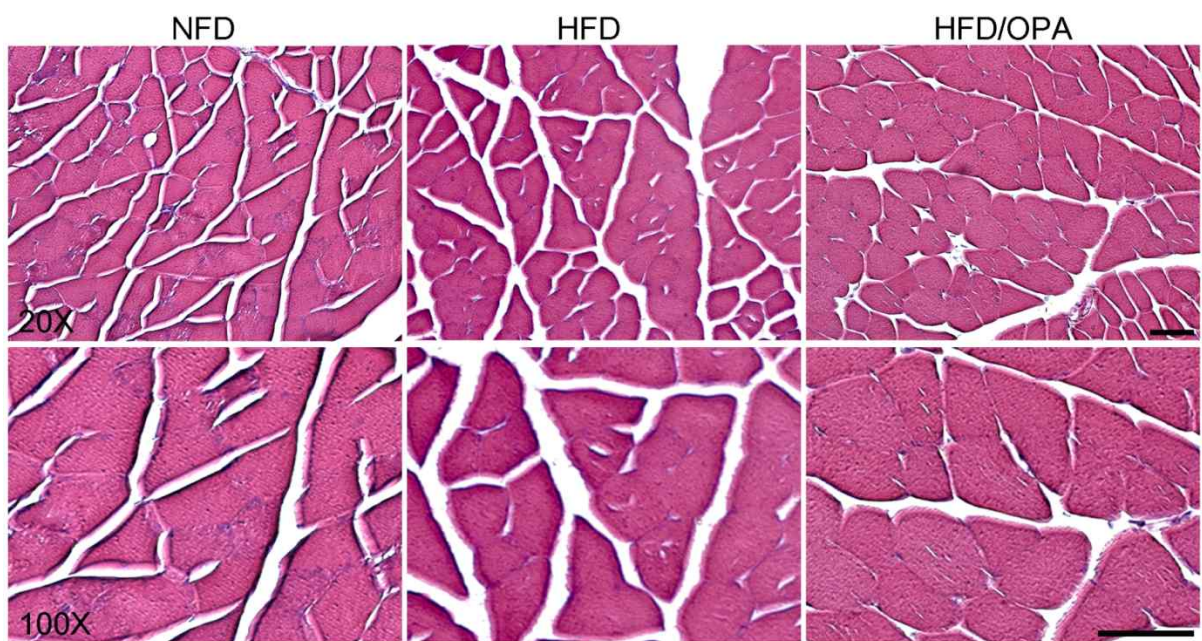


Fig. 3-14. Histological change of muscle tissues of C57BL/6J mice. Muscle tissues were stained using H&E method.

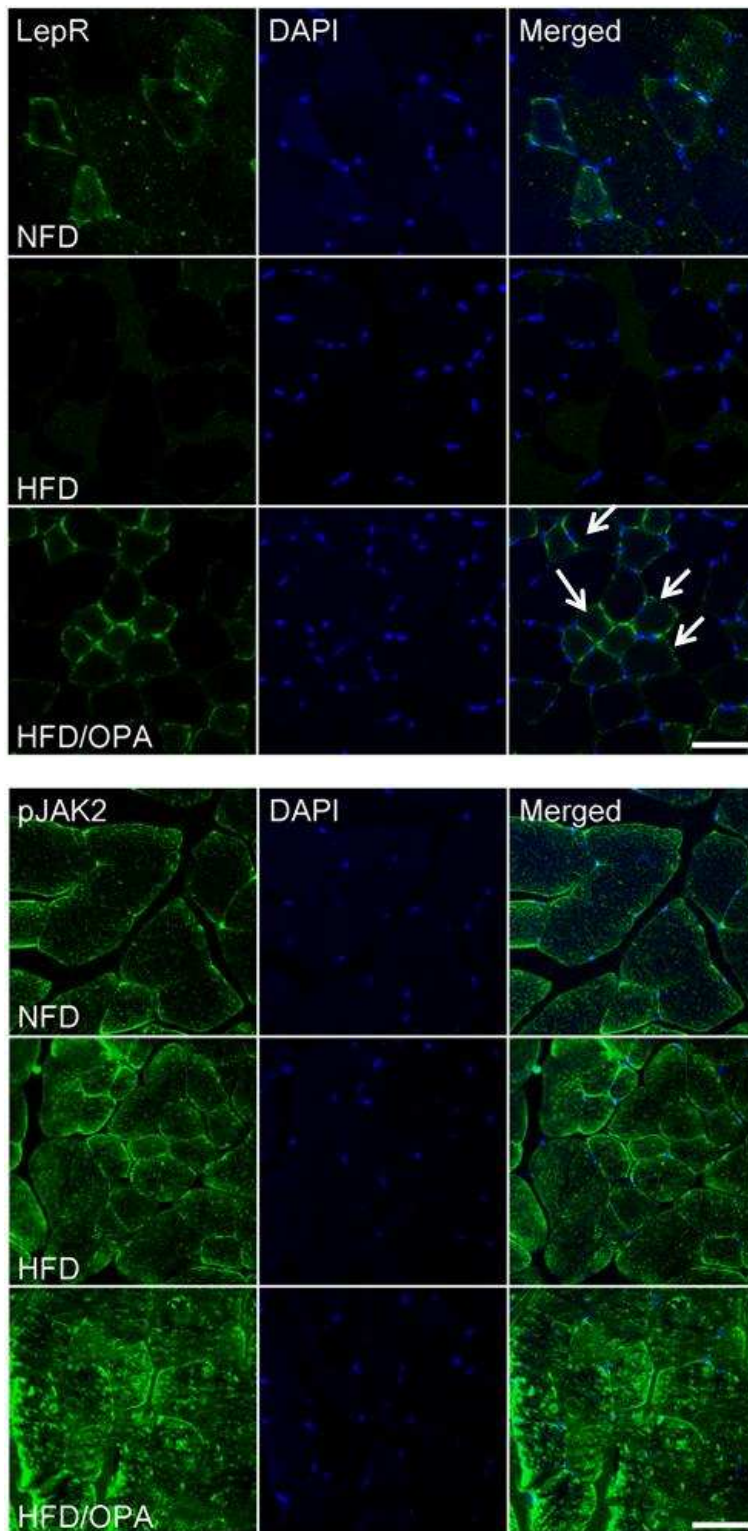


Fig. 3-15. Expression of leptin receptor and pJAK2 in muscle tissues of C57BL/6J mice. Muscle tissues were detected using immunohistochemistry.

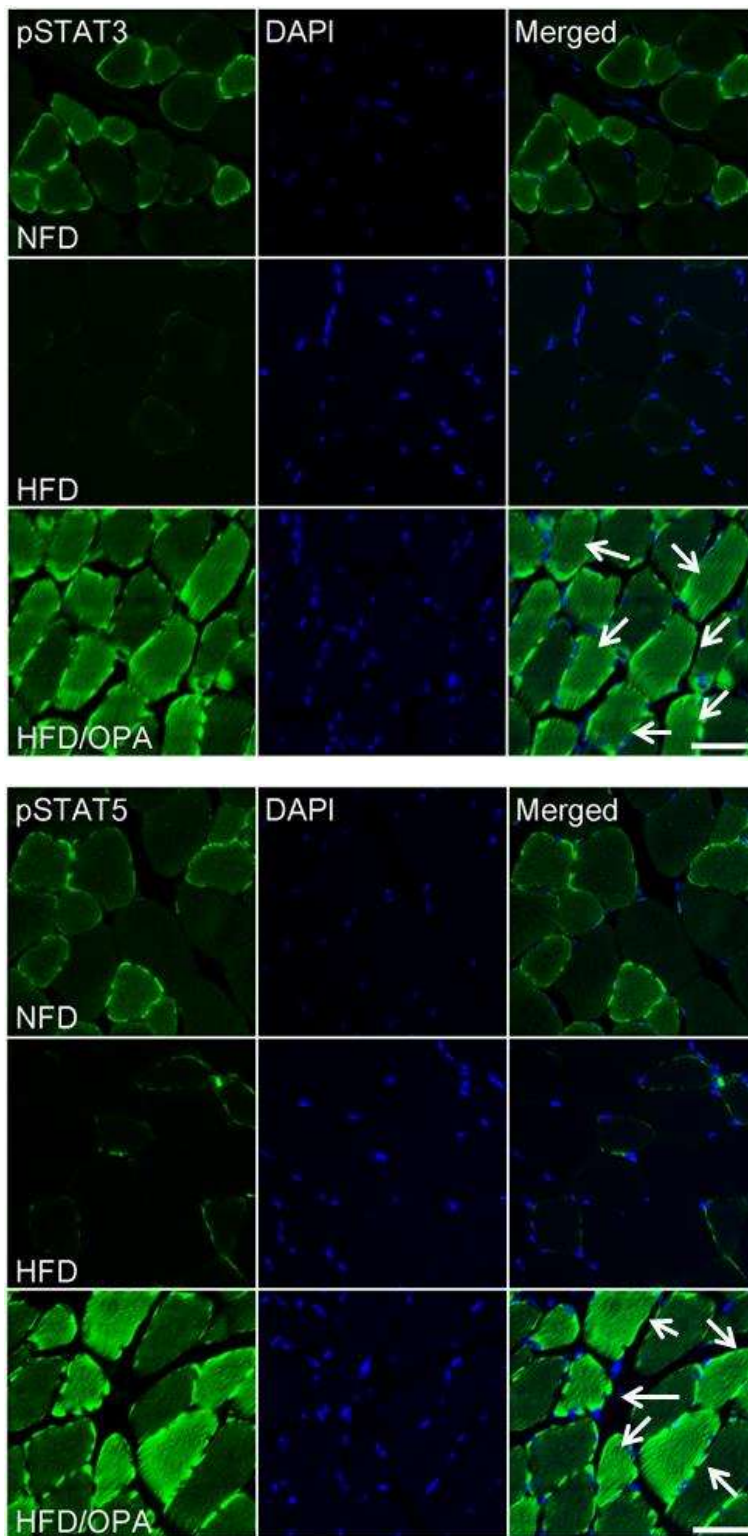


Fig. 3-16. Expression of pSTAT3 and pSTAT5 in muscle tissues of C57BL/6J mice.

Muscle tissues were detected using immunohistochemistry.

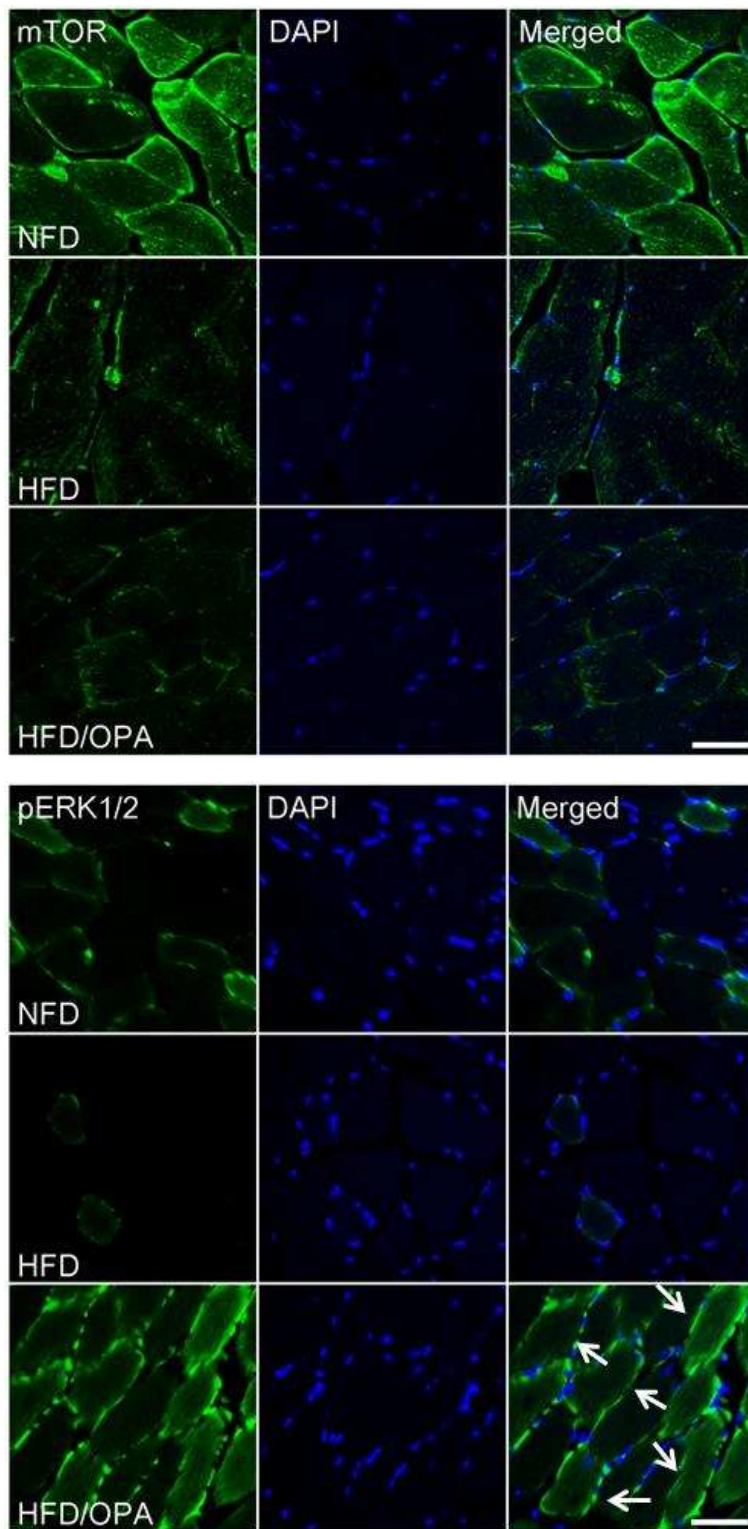


Fig. 3-17. Expression of mTOR and pERK1/2 in muscle tissues of C57BL/6J mice.

Muscle tissues were detected using immunohistochemistry.

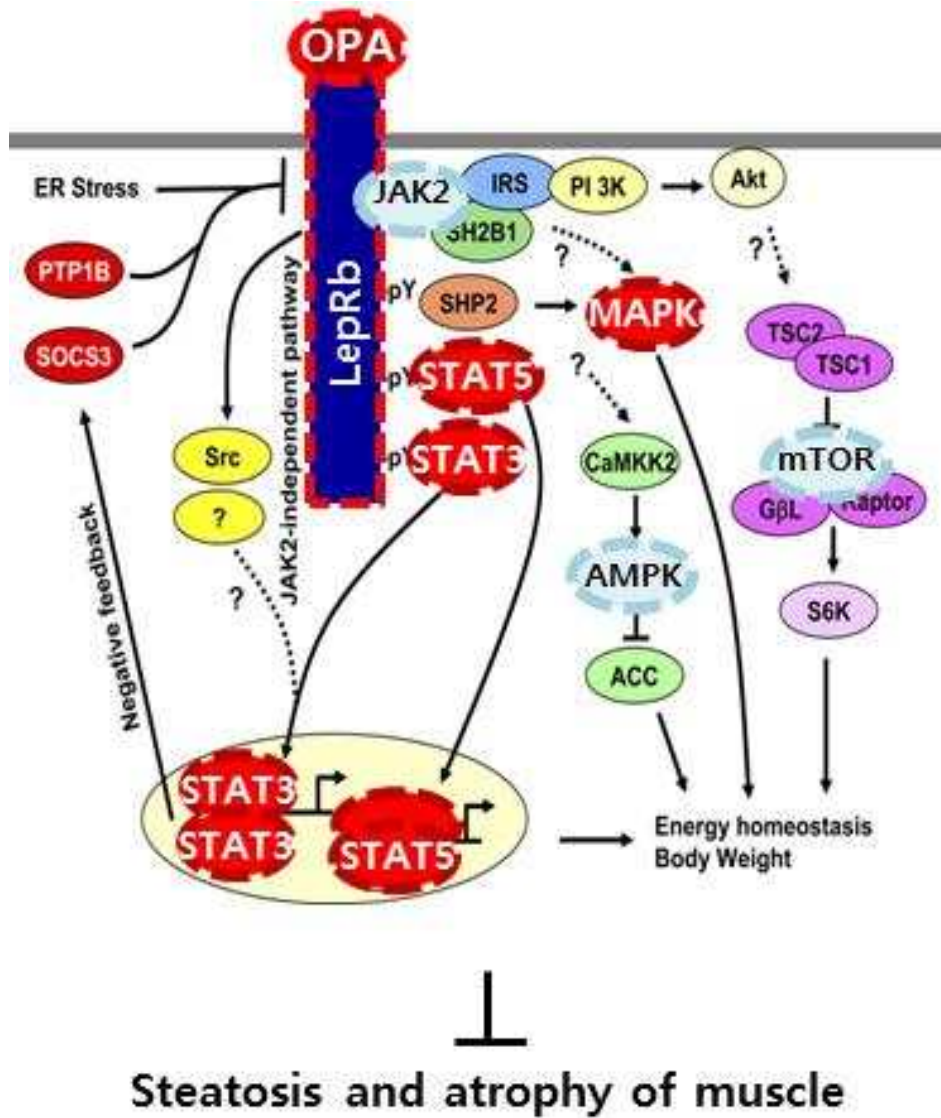


Fig. 3-18. Mechanism of OPA to leptin signal in muscle tissue of C57BL/6J mice.
 OPA directly affects glucose metabolism through phosphorylation of both STAT3 and STAT5.

CONCLUSION ON THIS STUDY

In this study, anti-obesity effect of OPA derived from *Ishige sinicola* through leptin signaling pathway was simulated in *in silico* and verified in *in vitro* and *in vivo*. OPA favorably docked to the leptin receptor. Also, OPA stimulated the leptin signaling pathway, including STAT5, in hypothalamic N1 neuron cell line. C57BL/6J obese mice treated with OPA showed reduced body weight and food intake compared to that observed in control obese mice. Furthermore, OPA stimulated leptin receptors, and activated phospho-STAT5 in the hypothalamic arcuate nucleus (ARC). Moreover, OPA activated leptin signaling in all peripheral tissues including white adipose tissues, liver, and muscle. It also reduced the fat size, hepatic steatosis, and regulated glucose metabolism. These results indicate that OPA, a marine-derived bioactive compound, regulates obesity through the leptin signaling pathway in both appetite control via the central nervous system and energy homeostasis via the peripheral nervous system in obese mice fed on a high-fat diet.

REFERENCE

2013 국민건강통계, 보건복지부

비만합병증 발생기전 이해와 임상적용 – 대사 질환, 김경아, 2015년 대한비만학회
춘계 연수강좌

비만치료 지침 2012, 대한비만학회

<http://www.who.int/mediacentre/factsheets/en/>

Balland, E., & Cowley, M. A. (2015). New insights in leptin resistance mechanisms in mice. *Frontiers in neuroendocrinology*, 39, 59-65.

Carter, S., Caron, A., Richard, D., & Picard, F. (2013). Role of leptin resistance in the development of obesity in older patients. *Clin Interv Aging*, 8, 829-844.

Chatterjee, S., Ganini, D., Tokar, E. J., Kumar, A., Das, S., Corbett, J., Kadiiska, M. B., Waalkes, M. P., Diehl, A. M., & Mason, R. P. (2013). Leptin is key to peroxynitrite-mediated oxidative stress and Kupffer cell activation in experimental non-alcoholic steatohepatitis. *Journal of hepatology*, 58(4), 778-784.

Crujeiras, A. B., Carreira, M. C., Cabia, B., Andrade, S., Amil, M., & Casanueva, F. F. (2015). Leptin resistance in obesity: an epigenetic landscape. *Life sciences*, 140, 57-63.

Ferreira, L. G., dos Santos, R. N., Oliva, G., & Andricopulo, A. D. (2015). Molecular docking and structure-based drug design strategies. *Molecules*, 20(7), 13384-

13421.

Frühbeck, G. (2002). Peripheral actions of leptin and its involvement in disease.

Nutrition reviews, 60(suppl 10), S47-S55.

Heo, S.-J., Hwang, J.-Y., Choi, J.-I., Han, J.-S., Kim, H.-J., & Jeon, Y.-J. (2009).

Diphlorethohydroxycarmalol isolated from *Ishige okamurae*, a brown algae, a potent α -glucosidase and α -amylase inhibitor, alleviates postprandial hyperglycemia in diabetic mice. *European journal of pharmacology*, 615(1), 252-256.

Heo, S.-J., & Jeon, Y.-J. (2009). Protective effect of fucoxanthin isolated from

Sargassum siliquastrum on UV-B induced cell damage. *Journal of Photochemistry and Photobiology B: Biology*, 95(2), 101-107.

Huynh, F. K., Neumann, U. H., Wang, Y., Rodrigues, B., Kieffer, T. J., & Covey, S. D.

(2013). A role for hepatic leptin signaling in lipid metabolism via altered very low density lipoprotein composition and liver lipase activity in mice. *Hepatology*, 57(2), 543-554.

Jung, U. J., & Choi, M.-S. (2014). Obesity and its metabolic complications: the role of

adipokines and the relationship between obesity, inflammation, insulin resistance, dyslipidemia and nonalcoholic fatty liver disease. *International journal of molecular sciences*, 15(4), 6184-6223.

Kamegai, J., Tamura, H., Shimizu, T., Ishii, S., Sugihara, H., & Wakabayashi, I. (2001).

Chronic central infusion of ghrelin increases hypothalamic neuropeptide Y and Agouti-related protein mRNA levels and body weight in rats. *Diabetes*, 50(11), 2438-2443.

- Kang, N., Lee, J.-H., Lee, W., Ko, J.-Y., Kim, E.-A., Kim, J.-S., Heu, M.-S., Kim, G. H., & Jeon, Y.-J. (2015). Gallic acid isolated from *Spirogyra* sp. improves cardiovascular disease through a vasorelaxant and antihypertensive effect. *Environmental toxicology and pharmacology*, 39(2), 764-772.
- Kim, A.-R., Shin, T.-S., Lee, M.-S., Park, J.-Y., Park, K.-E., Yoon, N.-Y., Kim, J.-S., Choi, J.-S., Jang, B.-C., & Byun, D.-S. (2009). Isolation and identification of phlorotannins from *Ecklonia stolonifera* with antioxidant and anti-inflammatory properties. *Journal of Agricultural and Food Chemistry*, 57(9), 3483-3489.
- Kim, K.-N., Yang, H.-M., Kang, S.-M., Ahn, G., Roh, S. W., Lee, W., Kim, D., & Jeon, Y.-J. (2015). Whitening Effect of Octaphlorethol A Isolated from *Ishige foliacea* in an In Vivo Zebrafish Model. *J. Microbiol. Biotechnol*, 25(4), 448-451.
- Kim, M.-M., Van Ta, Q., Mendis, E., Rajapakse, N., Jung, W.-K., Byun, H.-G., Jeon, Y.-J., & Kim, S.-K. (2006). Phlorotannins in *Ecklonia cava* extract inhibit matrix metalloproteinase activity. *Life sciences*, 79(15), 1436-1443.
- Klok, M., Jakobsdottir, S., & Drent, M. (2007). The role of leptin and ghrelin in the regulation of food intake and body weight in humans: a review. *Obesity reviews*, 8(1), 21-34.
- Ladenheim, E. E. (2015). Liraglutide and obesity: a review of the data so far. *Drug design, development and therapy*, 9, 1867.
- Lee, S.-H., Kang, S.-M., Ko, S.-C., Kang, M.-C., & Jeon, Y.-J. (2013). Octaphlorethol A, a novel phenolic compound isolated from *Ishige foliacea*, protects against streptozotocin-induced pancreatic β cell damage by reducing oxidative stress and apoptosis. *Food and chemical toxicology*, 59, 643-649.

- Lee, S.-H., Kang, S.-M., Ko, S.-C., Moon, S.-H., Jeon, B.-T., Lee, D. H., & Jeon, Y.-J. (2014). Octaphloretol A: a potent α -glucosidase inhibitor isolated from *Ishige foliacea* shows an anti-hyperglycemic effect in mice with streptozotocin-induced diabetes. *Food & function*, 5(10), 2602-2608.
- Li, Y.-X., Wijesekara, I., Li, Y., & Kim, S.-K. (2011). Phlorotannins as bioactive agents from brown algae. *Process Biochemistry*, 46(12), 2219-2224.
- Litwak, S. A., Wilson, J. L., Chen, W., Garcia-Rudaz, C., Khaksari, M., Cowley, M. A., & Enriori, P. J. (2014). Estradiol prevents fat accumulation and overcomes leptin resistance in female high-fat diet mice. *Endocrinology*, 155(11), 4447-4460.
- Marti, A., Berraondo, B., & Martinez, J. (1999). Leptin: physiological actions. *Journal of physiology and biochemistry*, 55(1), 43-49.
- Martin, R. L., Perez, E., He, Y.-J., Dawson, R., & Millard, W. J. (2000). Leptin resistance is associated with hypothalamic leptin receptor mRNA and protein downregulation. *Metabolism*, 49(11), 1479-1484.
- Meister, B. (2000). Control of food intake via leptin receptors in the hypothalamus. *Vitamins & Hormones*, 59, 265-304.
- Miranda, C. L., Elias, V. D., Hay, J. J., Choi, J., Reed, R. L., & Stevens, J. F. (2016). Xanthohumol improves dysfunctional glucose and lipid metabolism in diet-induced obese C57BL/6J mice. *Archives of biochemistry and biophysics*, 599, 22-30.
- Myers, M. G., Cowley, M. A., & Münzberg, H. (2008). Mechanisms of leptin action and leptin resistance. *Annu. Rev. Physiol.*, 70, 537-556.
- Park, H.-K., & Ahima, R. S. (2015). Physiology of leptin: energy homeostasis,

- neuroendocrine function and metabolism. *Metabolism*, 64(1), 24-34.
- Park, S. J., Kim, Y. T., & Jeon, Y. J. (2012). Antioxidant dieckol downregulates the Rac1/ROS signaling pathway and inhibits Wiskott-Aldrich syndrome protein (WASP)-family verprolin-homologous protein 2 (WAVE2)-mediated invasive migration of B16 mouse melanoma cells. *Molecules and cells*, 33(4), 363-369.
- Roujeau, C., Jockers, R., & Dam, J. (2014). New pharmacological perspectives for the leptin receptor in the treatment of obesity. *Frontiers in endocrinology*, 5, 167.
- Sáinz, N., Barrenetxe, J., Moreno-Aliaga, M. J., & Martínez, J. A. (2015). Leptin resistance and diet-induced obesity: central and peripheral actions of leptin. *Metabolism*, 64(1), 35-46.
- Sáinz, N., Rodríguez, A., Catalán, V., Becerril, S., Ramírez, B., Gomez-Ambrosi, J., & Frühbeck, G. (2010). Leptin administration downregulates the increased expression levels of genes related to oxidative stress and inflammation in the skeletal muscle of ob/ob mice. *Mediators of inflammation*, 2010.
- Wijesinghe, W., & Jeon, Y.-J. (2012). Exploiting biological activities of brown seaweed *Ecklonia cava* for potential industrial applications: a review. *International journal of food sciences and nutrition*, 63(2), 225-235.
- Yang, R., & Barouch, L. A. (2007). Leptin signaling and obesity cardiovascular consequences. *Circulation research*, 101(6), 545-559.
- Yang, Y.-I., Ahn, J.-H., Choi, Y. S., & Choi, J.-H. (2015). Brown algae phlorotannins enhance the tumoricidal effect of cisplatin and ameliorate cisplatin nephrotoxicity. *Gynecologic oncology*, 136(2), 355-364.
- Yuriev, E., Holien, J., & Ramsland, P. A. (2015). Improvements, trends, and new ideas

in molecular docking: 2012–2013 in review. *Journal of Molecular Recognition*, 28(10), 581-604.

Zabeau, L., Peelman, F., & Tavernier, J. (2015). Leptin: From structural insights to the design of antagonists. *Life sciences*, 140, 49-56.

Zhou, Y., & Rui, L. (2013). Leptin signaling and leptin resistance. *Frontiers of medicine*, 7(2), 207-222.